ISSI Book Title "The Delivery of Water to Proto-planets, Planets, and Satellites"

Chapter Title: Water and Volatile Inventories of Mercury, Venus, the Moon, and Mars

Authors: James P. Greenwood[1], Shun-ichiro Karato[2], Kathleen E. Vander Kaaden[3], Kaveh Pahlevan[4], and Tomohiro Usui[5]

Affilliations: [1]Department of Earth and Environmental Sciences, Wesleyan University, Middletown, CT 06459, USA, [2]Department of Geology and Geophysics, Yale University, New Haven, CT 06520, USA, [3]Jacobs, NASA Johnson Space Center, Mail Code XI3, Houston, TX 77058, USA, [4]School of Earth & Space Exploration, Arizona State University, Tempe, AZ, 85281, USA [5]Earth-Life Science Institute, Tokyo Institute of Technology, 2-12-1 Ookayama, Meguro, Tokyo 152-8550, Japan

Abstract– We review the geochemical observations of water, D/H and volatile element abundances of the inner Solar System bodies, Mercury, Venus, the Moon, and Mars. We focus primarily on the inventories of water in these bodies, but also consider other volatiles when they can inform us about water. For Mercury, we have no data for internal water, but the reducing nature of the surface of Mercury would suggest that some hydrogen may be retained in its core. We evaluate the current knowledge and understanding of venusian water and volatiles and conclude that the venusian mantle was likely endowed with as much water as Earth of which it retains a small but non-negligible fraction. Estimates of the abundance of the Moon's internal water vary from Earth-like to one to two orders of magnitude more depleted. Cl , K, and Zn isotope anomalies for lunar samples argue that the giant impact left a unique geochemical fingerprint on the Moon, but not the Earth. For Mars, an early magma ocean likely generated a thick crust; this combined with a lack of crustal recycling mechanisms would have led to early isolation of the Martian mantle from later delivery of water and volatiles from surface reservoirs or late accretion. The abundance estimates of Martian mantle water are similar to those of the terrestrial mantle, suggesting some similarities in the water and volatile inventories for the terrestrial planets and the Moon.

Table of contents

1. Introduction

Where did the Earth's oceans come from? This question is at the core of what motivates the study of the sources of water for inner Solar System bodies, and its answer will ultimately inform us on the sources and inventories of water in extrasolar planets. In this chapter, we will review the current knowledge regarding the abundances and sources of water for Mercury, Venus, the Moon, and Mars. We will primarily consider H and D/H, but will use other highly volatile elements (C, N, O, S, Cl) and their isotopes when they can inform us on the origins of water in the inner Solar System. Use of other common highly volatile elements is especially important when data on water for a body is poor or non-existent (as also occurs in the case of chondrites, e.g., the enstatite chondrites). This brings us to the problem of datasets for these four bodies. For Mercury, H data does not exist. For Venus, H data are only available for the upper atmosphere. For the Moon, H data exists for both the surface and interior, and for Mars a relative plethora of datasets on H abundance exist for the atmosphere, the surface, and the interior. Yet a glut of data does not guarantee an answer to the source of water delivery, as both the sources and inventory of Earth's water continue to be debated (e.g., Peslier et al., 2017; Genda and Ikoma, 2008; Halliday 2013; Marty, 2012; Marty et al., 2016, Hallis et al. 2015). In this chapter we will use 'water' to refer to total H, but H should be understood to be the sum of all species of hydrogen (H_2, H_2O, and OH). We will also discuss measurements of hydrogen using weight percent (wt.%) or parts per million (ppm wt) H_2O. The sources of water to the inner Solar System are discussed in the chapter by Alexander et al. (2018), and the delivery of water to the terrestrial planets is the subject of the chapter by O'Brien et al. (2018). The abundance and sources of terrestrial water are discussed in the complementary chapter by Peslier et al. (2017).

1.1. Gamma-ray spectroscopy of Mercury, Venus, the Moon, and Mars and their moderately volatile elements

Gamma-Ray Spectroscopy (GRS) collected by an orbiting spacecraft is the only measurement technique that has been employed on all four bodies, and its dataset is a useful starting point for this chapter. The GRS measurements acquired in the last decade at Mercury

completed this dataset for the four bodies (Figure 1 adapted from McCubbin et al., 2012a). In Figure 1, remote GRS data for the surfaces of Mercury, Venus, the Moon, and Mars are compared to estimates of the bulk silicate Earth (Kitts and Lodders, 1998; Lodders and Fegley, 1998; Lucey et al., 2006; McDonough and Sun, 1995; Peplowski et al., 2011; Taylor, 2013). Figure 1 shows an important result: while K, U, Th are all lithophile elements, K is also moderately volatile, while U and Th are refractory elements. An element's volatility is a direct reflection of its condensation temperature from a gas of solar composition (Wood et al., 2010). Under highly reducing conditions, K can become less volatile, but still more volatile than U and Th (Ebel and Sack, 2012). All three elements behave as similarly incompatible elements during planetary differentiation, meaning that they are not expected to fractionate from one another in the processes of magmatism and volcanism in the parent bodies. Figure 2a shows an abundance plot of another highly incompatible lithophile element, La, vs. U for Mars, Earth, the Moon, and the HED (howardite-eucrite-diogenite) meteorites that are believed to originate from 4 Vesta (McSween et al., 2013) demonstrating U and La are not fractionated from each other during planetary igneous processes. In Figure 2b, K is plotted vs. La for these same bodies. There is a systematic depletion in K in the order Mars, Earth, Vesta, and the Moon from the CI and LL chondrites (Fig. 2b). The depletions in K in the CV and CO chondrites are similar to Earth and Mars. This suggests that the depletion in K could be used as a proxy for a systematic depletion in all the volatile lithophile elements in these bodies relative to the Sun and CI chondrites.

In Figure 1, Mercury is as enriched in K as Earth, Mars, and Venus. Yet, Earth has oceans, and Mercury clearly does not. While this contrast may be related to the history of redox evolution, volatile processing, and atmospheric loss, it does raise the question: Do moderately volatile lithophile elements give us any information about the inventory of highly volatile elements, such as H, C, and N? When one considers the systematic depletion of K for the Moon and Vesta relative to Earth and Mars shown in Figures 1 and 2b, it would appear that K was subsequently lost to space or that these bodies accreted different amounts of K. Subsequent loss of K is quite plausible for the Moon and Vesta, which are believed to have had magma oceans that could have led to depletions in K (Wang and Jacobsen, 2016; Mandler and Elkins-Tanton, 2013). Loss of K during the Earth-Moon giant impact event might also explain why Mars is enriched relative to Earth. Mercury is at least similar in moderately volatile elements to Earth, which argues strongly against models such as the one proposed by Albarède (2009) that predict

that the volatile element chemistry of a body is related to its heliocentric distance when it formed. Thus, if Mercury is as enriched in K and other moderately volatile elements as the Earth, Venus, and Mars, it raises the question of whether Mercury accreted as much water as the Earth? Did Venus acquire as much water as Earth? And for that matter, what about Mars? Did Mars have *more* water than the Earth? Can moderately volatile elements be used as an indication of abundances of the highly volatile elements H, C, and N?

The similarity between Earth and Mars and CV and CO chondrites in Fig. 2b argues that this depletion in K could be due to accretion of K depleted material, rather than loss of K to space. Chondritic meteorites also show systematic depletions in moderately volatile elements as shown in Figure 3a-f. Here the moderately and highly volatile elements are shown vs. 50% condensation temperature for three types of carbonaceous chondrites (CM, CO, CV), the LL ordinary chondrites, and EL and EH enstatite chondrites, normalized to CI chondrite and Si. All classes of chondrite show depletions in the moderately and highly volatile elements relative to CI chondrite. The cosmochemical affinities of the elements are also shown, and the three carbonaceous chondrites exhibit a systematic depletion of elements with decreasing condensation temperature, regardless of whether the elements are siderophile, chalcophile, or lithophile, suggesting that these volatile element depletions are nebular in origin, as planetary differentiation would fractionate siderophile and chalcophile from lithophile elements during core formation (Wood et al. 2010).

1.2 Highly volatile and moderately volatile element depletions of the chondrites

The volatile elements H, C, and N are also plotted in Figure 3, and the abundances of these three highly volatile elements are also strongly depleted in the chondrites. While some of this depletion may be due redistribution of elements during metamorphism, there appears to be a systematic depletion trend in the volatile elements for each type of chondrite shown in Figure 3. The CM chondrites have overall higher abundances of volatiles than the other chondrite groups shown, and appear slightly enriched compared to their moderately volatile element depletion trend. The other three chondrite groups have H, C, and N abundances that appear to plot close to an extension of their moderately volatile element depletion trend. The LL chondrites have a strong depletion in the siderophile and chalcophile elements, while being quite high in H, C, and

N (Alexander et al., 2012), as well as being high in moderately volatile lithophile elements, such as K. There are no primitive enstatite chondrites (EC), and thus they are also affected by metamorphism. The ECs retain significant C and N demonstrating that they have not suffered complete loss of volatiles as is sometimes thought (H has not been reliably measured in ECs; e.g., Jarosewich, 1990). If the volatile element abundances of the chondrites plot on an extension of their moderately volatile element depletion trends in Fig. 3, this would suggest that whatever processes caused the moderately volatile element depletions in chondrites and the inner Solar System bodies may also be responsible for the depleted abundances of the highly volatile elements (H, C, N) in these bodies.

Thus, the chondrites point to the commonality of moderately volatile element depletions between the differentiated inner Solar System bodies Mercury, Venus, the Moon, Mars, and Vesta and the undifferentiated chondrites, and demonstrates an early loss of volatile elements *prior* to planetary differentiation. The chondrites also demonstrate that the highly volatile element abundances may reflect the processes that caused moderately volatile element depletions of these different inner Solar System bodies and materials. The processes that caused the systematic depletion trends in the moderately volatile lithophile elements are likely to be high temperature processes, such as condensation or evaporation of rock components (Young, 2017). These high temperature processes are likely to significantly deplete the volatile elements H, C, N, as well as the noble gases of the precursor materials for Mercury, Venus, Earth-Moon, and Mars, and have led to the prevailing ideas that highly volatile elements were completely lost during the processes that caused the moderately volatile element depletions, and then were added back to the Earth and the other inner Solar System bodies at some later time (e.g. Albaréde, 2009). By contrast, the abundances of H, C, and N in primitive CV, CO, and CM chondrites appear to be similar to their expected depletions from an extension of the trend of their depletions in moderately volatile elements to lower temperatures. The enstatite chondrites have quite substantial abundances of C and N (Grady et al., 1986). If Earth's precursor materials were similar to ECs, this would imply that some fraction of the highly volatile elements were inherited from the local nebular environment of inner Solar System bodies, rather than being completely lost during planetary accretion, and then delivered later by chondritic asteroids or comets.

2. Water, D/H, and volatile elements of Mercury, Venus, Moon, and Mars

2.1. Mercury

2.1.1. Introduction

Prior to the return of data from the MErcury Surface, Space ENvironment, GEochemistry and Ranging (MESSENGER) spacecraft (Solomon et al., 2001), the planet Mercury was thought to be depleted in volatile elements primarily due to its close proximity to the Sun (Albarède, 2009). Initial analyses conducted during flybys from the Mariner 10 mission confirmed the presence of exospheric H, He, and O (Broadfoot et al., 1974; Broadfoot et al., 1976). Furthermore, ground-based discoveries enhanced our knowledge about Na, K, and Ca in the exosphere (Bida et al., 2000; Potter and Morgan, 1985, 1986), as well as polar volatiles found in radar-reflective deposits (Harmon and Slade, 1992; Slade et al., 1992). Despite this evidence for the presence of volatiles on the surface of the planet and in the exosphere, it was not until the return of data from MESSENGER that it was discovered just how volatile-rich Mercury is (Evans et al., 2015; McCubbin et al., 2012a; Murchie et al., 2015; Nittler et al., 2011; Peplowski et al., 2014; Peplowski et al., 2016; Peplowski et al., 2015; Peplowski et al., 2012; Weider et al., 2012).

Among the numerous instruments onboard MESSENGER, the X-Ray Spectrometer (XRS), Gamma-Ray Spectrometer (GRS), and Neutron Spectrometer (NS) have provided the greatest amount of information regarding the volatile content of Mercury (Evans et al., 2015; Evans et al., 2012; Lawrence et al., 2013; Nittler et al., 2011; Peplowski et al., 2014; Peplowski et al., 2016; Peplowski et al., 2015; Peplowski et al., 2012). These data have shown that the surface of the planet has elevated abundances of C (Murchie et al., 2015; Peplowski et al., 2016; Peplowski et al., 2015), Na (Peplowski et al., 2014), S (Nittler et al., 2011; Weider et al., 2012), Cl (Evans et al., 2015), and K (Peplowski et al., 2012), likely indicating that Mercury has high levels of indigenous volatiles. Additionally, although a likely exogenic component, elevated H has been seen in the polar regions compared to other portions of the planet's surface (Lawrence et al., 2013). Furthermore, elevated K/Th and near chondritic K/Cl ratios at Mercury's surface lends support to the volatile-rich nature of the planet (Evans et al., 2015; McCubbin et al., 2012a; Peplowski et al., 2011; Peplowski et al., 2012). Although not considered a volatile element, MESSENGER XRS data has also shown that the surface of the planet is depleted in Fe (Nittler et al., 2011; Weider et

al., 2012). These characteristic elemental abundances have facilitated calculation of the oxygen fugacity (fO_2) characterizing silicate Mercury, which is between 2.6 and 7.3 $\log_{10}$ units below the iron-wüstite buffer (McCubbin et al., 2017; McCubbin et al., 2012a; Zolotov et al., 2013; Zolotov et al., 2011), making Mercury the most reduced terrestrial planet (Herd, 2008; Sharp et al., 2013; Wadhwa, 2008).

2.1.2. Pyroclastic Deposits

Pyroclastic deposits across the surface of Mercury have been identified by their characteristic diffuse borders, high reflectance compared to nearby units, and a steeper slope in their reflectance spectrum from visible to near-infrared wavelengths (Blewett et al., 2009; Kerber et al., 2011; Kerber et al., 2009; Rava and Hapke, 1987; Robinson et al., 2008). On Mercury, 51 pyroclastic deposits have been identified from the MESSENGER data, covering >111,000 km^2 of the mercurian surface, or ~0.15% of the total surface (Goudge et al., 2014; Kerber et al., 2011). Of these 51 deposits, >90% of them are located within impact craters and basins (Goudge et al., 2014). The pyroclastic deposits on Mercury are larger than pyroclastic deposits found on the Moon, suggesting that they involved higher energy eruptions with more abundant volatiles from the interior of the planet than what was typically associated with lunar pyroclastic eruptions (Kerber et al., 2011; Thomas et al., 2015). Furthermore, although the majority of pyroclastic deposits on Mercury are located away from the smooth plains, there are pyroclastic deposits associated with the margins of some smooth plains units, analogous to lunar pyroclastic deposits that are adjacent to lunar maria (e.g., Goudge et al., 2014, Head and Wilson 1979). Thomas et al., (2014) presented evidence suggesting that the pyroclastic eruptions initially occurred ~3.9 Ga and continued until less than a billion years ago. This long duration of explosive volcanism suggests that large amounts of volatiles are present in the mercurian interior. Kerber et al. (2011) calculated CO abundances of 1600–16000 ppm wt are required if the pyroclastic eruptions on Mercury are similar to Hawaiian-style eruptions on Earth. Given the reduced nature of the planet, as revealed by MESSENGER, Kerber et al. (2011) proposed S_2Cl, Cl, Cl_2, and COS as the possible driving forces behind mercurian pyroclastic eruptions. Given the highly reducing nature of the planet, it is also possible that H_2 or H_2S are present and could have aided in driving these pyroclastic eruptions.

256 *2.1.3. Magmatic Volatiles and the Evolution of Mercury*

257

258 The role that volatiles played in the thermal and magmatic evolution of Mercury are critical
259 to understanding the present-day planet as investigated by Mariner 10 and MESSENGER.
260 Although all of the chemical analyses currently obtained for Mercury are solely of surface
261 compositions, these data have been used to infer the abundance of volatiles in the mercurian
262 interior (Evans et al., 2015; Malavergne et al., 2004; Malavergne et al., 2010; Namur et al., 2016;
263 Stockstill-Cahill et al., 2012; Vander Kaaden and McCubbin, 2015, 2016; Zolotov et al., 2013;
264 Zolotov et al., 2011).

265 In Mercury, C is thought to be present in the form of elemental C as opposed to CO or CO_2.
266 Initially, GRS measurements placed C abundance of Mercury's surface at 1.4 ± 0.9 wt.%
267 (Peplowski et al., 2015). At the 3-sigma standard deviation level, this allowed for C abundances
268 on Mercury to be between 0 wt.% and 4.1 wt.%. Additional analyses using the NS on
269 MESSENGER showed C abundances on Mercury in the low reflectance material to be as high as
270 1–3 wt.% greater than the surrounding, higher reflectance materials (Peplowski et al., 2016). This
271 elevated C signature found in the low reflectance material on the planet's surface is likely due to
272 the presence of graphite, possibly from an ancient primary floatation crust (Murchie et al., 2015;
273 Vander Kaaden and McCubbin, 2015).

274 Other magmatic volatiles present in the mercurian interior include Na, Cl, and K. These
275 three elements are all higher in the north polar region of Mercury, where the largest volcanic unit
276 on the planet is located. This suggests that these volatiles played a role in the transport and eruption
277 of flood volcanics on Mercury. Given the low fO_2 of Mercury, S is likely present in the form of
278 sulfides instead of sulfates. Analogue and experimental studies have suggested the presence of Fe-
279 , Cr-, Mn-, Ti-, Mg-, Ca-bearing sulfides on Mercury (Malavergne et al., 2014; McCoy et al., 1999;
280 Namur et al., 2016; Vander Kaaden and McCubbin, 2016; Vander Kaaden et al., 2017; Zolotov et
281 al., 2013). It has also been suggested that a sulfide-rich conductive lid could have formed during a
282 mercurian magma ocean event (Parman et al., 2016). However, it is unlikely that pure CaS, which
283 is the only sulfide solid or immiscible melt that has been shown to be buoyant in a mercurian
284 magma ocean, would form given the preferential formation of MgS to CaS as well as the likely
285 formation of multi-component sulfides as opposed to single component sulfide phases (Vander
286 Kaaden and McCubbin, 2016).

Although the exact accretion history of Mercury is still debated, it is generally believed that Mercury experienced a giant impact that stripped much of its silicate mantle (Benz et al., 1988) and led to a magma ocean (Brown and Elkins-Tanton, 2009; Riner et al., 2009). The highly reducing conditions that were present in this magma ocean may have further contributed to the large mass of the metallic core reforming after the giant impact. However, given the geophysical data from MESSENGER, the density of the mercurian core – like the terrestrial core – requires addition of a light element component in addition to Fe (Hauck II et al., 2013; Smith et al., 2012). The most likely light element to make up this density difference, due to the low fO_2 and experimental results, is Si (Chabot et al., 2014a; Hauck II et al., 2013). With increasing Si contents in the mercurian core, C and S would both be excluded from it. Although S would preferentially partition into the silicate portion of the planet, C is also not soluble in the mercurian mantle, adding to exotic crust formation processes on the planet (Chabot et al., 2014a; Vander Kaaden and McCubbin, 2015; Vander Kaaden et al., 2016). Furthermore, based on experimental results at reducing conditions similar to Mercury, Na, Cl, and K are expected to preferentially partition into the silicate portion of the planet as well (Vander Kaaden and McCubbin, 2016). Following the results of Vander Kaaden and McCubbin (2015), this graphite would float to the surface of the magma ocean producing a primary graphite floatation crust, similar to the anorthositic crust exposed on the Moon.

Continued cooling of the planet would have resulted in the crystallization of the magma ocean. Analogous to the lunar magma ocean (Warren, 1985), the crystallizing cumulates would sink to the base of the magma ocean, enriching the melt in highly incompatible elements. However, due to the low fO_2 of the planet, and associated low FeO contents of mantle cumulates, solid-state overturn, which occurs in the lunar scenario, is not expected on Mercury (Vander Kaaden and McCubbin, 2015). Instead, the stratified mantle would reflect the bottom-up crystallization of the magma ocean, including volatile-rich phases, such as albitic plagioclase and possibly sodalite.

After crystallization of the magma ocean, continued volcanism on Mercury would have resurfaced the planet and buried the evidence of the primary graphite floatation crust (Vander Kaaden and McCubbin, 2015). The elevated abundances of S on the surface of Mercury, therefore, are the direct result of transport within reducing magmas that have a higher carrying capacity for S compared to moderately reduced to oxidized magmas (e.g., Tuff et al. 2013). Furthermore, the elevated abundances of Na, Cl, and K on the surface were most likely produced in a similar manner

given their lithophilic nature under mercurian oxygen fugacities (Vander Kaaden and McCubbin, 2016). Continued resurfacing of the planet through impacts, flood volcanism, and pyroclastic volcanism resulted in partial to total destruction of the primary graphite floatation crust and mixing with surface materials, darkening the reflection of the planet. Additional impacts have exposed evidence of this primary graphite floatation crust in the low reflectance material on the planet (Peplowski et al., 2016; Vander Kaaden and McCubbin, 2015). Finally, additional impacts from volatile-rich asteroidal material as well as comets have resulted in polar volatile deposits, which are mainly composed of water ice (Chabot et al., 2014b; Lawrence et al., 2013).

2.2. Venus

2.2.1. Introduction

Although Venus and the Earth have long been considered planetary "twins", Venus does not have plate tectonics. Instead, 92% of its surface has the same crater density, suggesting the same age of ~300–700 Ma (Schaber et al., 1992; McKinnon et al., 1998). Models suggest that episodic overturn of the mantle on this timescale leads to catastrophic resurfacing of the planet (Parmentier and Hess, 1992). The venusian atmosphere has Earth-like inventories of C and N, with terrestrial isotopic compositions, suggesting a primordial volatile inventory endowment not unlike Earth. In contrast, the modern atmosphere only has ~30 ppm wt H_2O, with a D/H ~150 times greater than the Earth's oceans (Fegley, 2014). This high D/H led to the suggestion that Venus originally had Earth-like levels of water, with a similar isotopic composition to the Earth's oceans, and that the majority of this water was subsequently lost to space (Ingersoll, 1969, Donahue et al., 1982). Models of this process suggest that such early loss scenarios would leave Venus with an initial water endowment of ~a few percent of a terrestrial ocean mainly held in the primitive venusian mantle (Hamano et al. 2013).

Elkins-Tanton et al. (2007) show that volcanism and volatile element recycling will likely never fully deplete the venusian mantle of volatiles. Thus, if atmospheric N and C could serve as proxies for primordial planetary water content, and if current scenarios for Venusian evolution have predictive value, then Venus can have ~0.01-0.1 times the terrestrial water inventory in its interior. If the majority of the interior water is released episodically during catastrophic

resurfacing events, the high D/H and low water content of the atmosphere could be explained via loss of water with an initially terrestrial isotopic composition to space on a 0.5–1.0 Ga timescale (Grinspoon, 1993).

2.2.2. Volatiles in the venusian atmosphere

The Venus atmosphere has high levels of CO_2, N_2, SO_2, HCl, and HF (Fegley, 2014). The abundance of C in Venus' atmosphere is similar to the crustal C inventory of the Earth (Fegley, 2014). The N abundance of Venus's atmosphere is several times higher than that of Earth's atmosphere, and two times higher than the total inventory of N in Earth's atmosphere, biosphere, oceans, and crust (Lodders and Fegley, 1998). The high level of SO_2 in the venusian atmosphere is 220 times lower than the Earth's total sulfur inventory in the crust and oceans, suggesting that there is abundant sulfur in the venusian crust and/or mantle. Hydrogen chloride and HF appear to be buffered by reactions with surface minerals (Fegley, 2014), most likely phosphate minerals such as apatite [$Ca_5(PO_4)_3F,Cl,OH$] (Treiman et al., 2016a). The presence of these atmospheric gases are believed to be the product of volcanic outgassing.

2.2.3. Water and volatile elements in the venusian mantle

Elkins-Tanton et al. (2007) showed that volatiles, such as water and CO_2, can partition into anhydrous mantle minerals during partial melting processes on Venus and other planetary bodies, and thus be partially retained in the mantle regardless if the mantle region is unmelted or has been previously involved in a melting event. They predict that some fraction of volatile elements will be retained in the venusian mantle, ranging from 100% in mantle regions that have not been melted at all, to 1–2% in regions that have experienced melting. They also argue that volatile-enriched lithosphere would be involved in crustal delamination processes in the thick venusian crust, and envision a way to reintroduce volatiles back into the mantle much the same way that plate tectonics on Earth re-fertilizes the mantle in volatiles.

High levels of unstable sulfur species in the venusian atmosphere argue for a replenishment mechanism by volatile input via volcanic degassing (Fegley, 2014). As Venus is similar in size to the Earth, it is likely to be just as volcanically active as the Earth, providing a

reasonable explanation for the venusian atmospheric sulfur contents and species (e.g., Fegley, 2014). Thus, if volcanic outgassing is responsible for the input of sulfur, then it is likely that other volatiles, such as C, N, and water are being supplied to the venusian atmosphere as well. The input of volatiles to the venusian atmosphere may be episodic, and at maximum abundance levels at the end of mantle overturn events that resurface the planet. The abundances of some volatiles in the atmosphere would then decline over time due to weathering reactions with crustal rocks (e.g., S, Cl) and loss and escape processes from the upper atmosphere (e.g., H), until the next mantle overturn event (on a timescale of ~0.5 to 1 Ga). Atmospheric species that do not react with surface rocks or are lost to space would accumulate (e.g., C, N, and Ne). Alternatively, volcanic outgassing is mostly quiescent, and steadily supplying volatiles to the venusian atmosphere over time (albeit with higher levels during and after mantle overturn events). A schematic of these various processes is shown for water in Figure 4 (modified from Gilmore et al., 2017).

2.2.4. Timing of water and volatile delivery and sources of water to Venus

The similarity in the isotopic ratios and abundances of the major volatiles C and N between the venusian atmosphere and Earth argues for a similar origin of volatiles for these two bodies. The extraordinarily high D/H of water in the venusian atmosphere argues strongly for loss of extensive amounts of water, such as an ocean's worth (Donahue, 1982) or more. The only other source of hydrogen known to have D/H similar to Venus are water and organics of the interstellar medium. It has been argued that delivery of cometary water followed by loss of water from the atmosphere through time could explain the elevated D/H of the Venus atmosphere (Grinspoon and Lewis, 1988). While comets are undoubtedly a source of water to the inner Solar System bodies, it is not necessary to advocate for this model today due to the expected high levels of volatiles in the venusian mantle (Elkins-Tanton et al., 2007). Loss of atmospheric water either from an early ocean world (Ingersoll, 1969, Donahue, 1982, Kasting and Pollack, 1983), or through episodic inputs of water due to mantle overturn with subsequent fractionation of D/H and loss of hydrogen from the upper atmosphere (Grinspoon, 1993), can explain the D/H systematics of Venus.

411 **2. 3. The Moon**

412

413 A major paradigm shift in our understanding of the lunar volatile inventory occurred with
414 a Secondary Ion Mass Spectrometry (SIMS) study of H_2O, CO_2, F, S, and Cl in lunar volcanic
415 glasses by Saal et al. (2008). They measured 4–46 ppm wt H_2O in lunar volcanic glasses. While
416 these are low values compared to terrestrial arc volcanic glasses, the lunar glasses are believed to
417 have undergone significant degassing during lunar fire-fountaining activity. Saal et al. (2008)
418 modeled a diffusive loss of volatiles during eruption to arrive at pre-eruptive volatile estimates of
419 260–745 ppm wt H_2O for a lunar green glass bead (a very low-Ti glass). These levels of water
420 are similar to water contents in mantle source regions of the Earth, such as mid-ocean ridge
421 basalts (MORBs) and Hawaiian ocean island basalts (OIBs) (Luth, 2005). This remarkable result
422 suggests that the Moon was able to retain water after the giant impact, or that water was accreted
423 shortly thereafter (Saal et al., 2008).

424 Much higher levels of indigenous lunar water have been found in the mineral apatite with
425 three separate SIMS studies finding 1000's of ppm wt OH in this phosphate mineral from rock
426 samples returned by the Apollo astronauts (Boyce et al., 2010; McCubbin et al., 2010a,b;
427 Greenwood et al., 2011). These high hydroxyl contents were far above background levels of at
428 most 10's of ppm, and could not be ascribed to terrestrial contamination. The three groups all
429 used different SIMS instruments, techniques, and standard terrestrial apatite minerals, but
430 obtained similar results for the H contents of lunar apatites (Boyce et al., 2010; McCubbin et al.,
431 2010a,b; Greenwood et al., 2011). The high OH contents of lunar apatites also confirmed the
432 results of Saal et al. (2008) that the Moon and its samples still retain some indigenous water
433 (Boyce et al., 2010; McCubbin et al., 2010a,b; Greenwood et al., 2011).

434 Since these early pioneering studies, a number of other research groups have embarked
435 on measuring the water contents and D/H of the Moon. A comprehensive review of lunar volatile
436 elements and their isotopes is provided by McCubbin et al. (2015a), and will not be restated here.
437 We will primarily review the evidence for 'water' and D/H in the Moon, but will also discuss
438 other volatiles as appropriate. The current state of our understanding of water and D/H in
439 different lunar reservoirs and sample types will be discussed after we consider issues associated
440 with the measuring of hydrogen contents in nominally anhydrous minerals from extraterrestrial
441 samples.

442

443 *2.3.1. Considerations for SIMS measurements of D/H and H in nominally anhydrous*
444 *extraterrestrial materials*

445

446 **SIMS.** SIMS measurements allow for accurate and precise measurements of small sample
447 volumes to be attained for D/H, if terrestrial contamination can be minimized, and is the primary
448 means by which meteorite and returned sample D/H is analyzed today. Detailed reviews of the
449 use of SIMS can be found in Hauri et al. (2002), Greenwood et al. (2011), Barnes et al. (2013),
450 Slodzian et al. (2014), and references therein. In brief, SIMS measurements involve the use of a
451 primary ion beam to sputter/excavate a small sample mass from a material's surface. The
452 'secondary ions' sputtered from the surface are then accelerated and collimated by electrostatic
453 lenses and filters before being separated according to mass using a large magnet, and then
454 collected/counted on one or more electronic multipliers or faraday cups, or with a SCAPS
455 (Stacked CMOS-type Activated Pixel Sensor) detector (Hokkaido University and University of
456 Hawaii SIMS machines) (Yurimoto et al., 2003). Removal of terrestrial adsorbed water from the
457 surfaces and near-surface region of the samples is accomplished by pumping of the sample under
458 high vacuum (>10^{-8} torr) for several days prior to analysis, and pre-sputtering the area to be
459 analyzed by rastering the primary ion beam over it (a form of ion milling) to remove the topmost
460 exposed surface of the sample (~ <1 μm). For D/H measurements, the secondary ions must be
461 extracted from the center of the secondary ion beam, to avoid contaminant water that will
462 condense in the outer regions on the edge of the secondary ion beam. A liquid N_2 cold trap can
463 also be used to trap contaminant water in the vacuum of the sample chamber. Contaminant water
464 will condense if any instrument components contact the secondary ion beam. This points to
465 difficulty of using NanoSIMS instruments to make D/H measurements of low-water containing
466 materials, as this instrument's immersion lens contacts the secondary ion beam, and will likely
467 lead to an endemically higher background of contaminant water during analyses. For these
468 reasons, in this chapter we will adopt a 'red light/yellow light/green light' approach to SIMS data
469 collected on extraterrestrial materials via mass spectrometry or SIMS for the interpretation of
470 D/H measurements. Below 50 ppm wt H_2O, this is the "red zone" wherein D/H measurements
471 are likely to be affected most strongly by terrestrial contamination. We will not consider D/H
472 data below 50 ppm wt H_2O in this chapter. We define the "yellow zone" as 50–150 ppm wt

H_2O, wherein caution should be applied when considering the interpretations of this data. We will alert the reader when we consider data in this range of water contents. Above 150 ppm wt H_2O is the "green zone", and data above this water content is generally excellent, though SIMS analyses that overlap onto cracks loaded with terrestrial contamination can still give extraterrestrial δD values (Greenwood et al., 2008). Thus, even above 150 ppm wt H_2O, caution must be exercised in the interpretation of D/H values in heavily shocked meteorites and returned samples, as the density of fractures can make finding an analytical area free of cracks (and thus reasonably free of terrestrial contamination) in the phase of interest quite challenging. An example of the difficulty in measuring water in extraterrestrial materials can be seen in a ^1H image of apatite from the Shergotty meteorite in Figure 5.

Cosmic Ray Exposure (CRE) corrections for D/H. Freidman et al. (1971) first measured elevated δD of 307‰ in basalt 12051, and proposed this to be a mixture of D-rich spallogenic H generated by cosmic rays and terrestrial contamination. Mare basalt 12051 has large grains of apatite (J. Greenwood, unpubl. data), and most apatite in mare basalts have 100's to 1000's of ppm wt OH with elevated δD (McCubbin et al., 2010a,b; Boyce et al, 2010; Greenwood et al., 2011; Tartése and Anand, 2013; Barnes et al., 2013, 2014; Tartése et al., 2013, 2014a,b), suggesting that rather than spallogenic deuterium, Freidman et al. (1971) measured a mixture of indigenous lunar hydroxyl from apatite and terrestrial contamination. This is relevant, because most of the H isotopic data in the literature (Saal et al., 2013; Barnes et al., 2013, 2014; Tartése and Anand (2013); Tartése et al., 2013, 2014a,b; Füri et al., 2014; Robinson and Taylor, 2014; Robinson et al., 2016) have been corrected for CRE using the deuterium production rate of Merlivat et al. (1976). Merlivat et al. (1976) derived their deuterium production rate from their stepped heating of basalt 70215, arguing that the majority of the hydrogen released at low temperature was terrestrial contamination, but that spallogenic H dominated the high temperature steps. Mare basalt 70215 is a fine-grained, rapidly cooled sample, and the apatite in it is sub-micron in size (J. Greenwood, unpubl. data). This suggests that Merlivat et al. (1976) did not measure spallogenic deuterium, but rather high δD associated with OH in apatite (e.g., Greenwood et al., 2011).

Füri and Deloule (2016) have derived a new D production rate for lunar samples, from careful analysis of olivine grains in lunar samples with varying CRE ages. The D-production rate

504 they define is 3x higher than that of Merlivat et al. (1976), but is in good agreement with the
505 theoretical D-production rate of Reedy (1981). The much higher D-production rate has important
506 consequences for a number of published lunar studies of D/H. For example, Hauri et al. (2017)
507 point out that in their own dataset for the pyroclastic glass beads of Saal et al. (2013), the
508 positive correlation of δD with decreasing water content they report (the expected trend of D/H
509 fractionation during degassing of H_2 gas (e.g., Sharp et al., 2013)), would produce a *negative*
510 correlation of δD with decreasing water content if they use the D-production rate of Füri and
511 Deloule (2016). This has profound implications if true: a negative correlation of δD with
512 decreasing water content can only occur by the degassing of molecular water (Taylor, 1986). As
513 molecular water is not the dominant hydrogen species at the low fO_2s expected of lunar magmas
514 (Hirschmann et al., 2012), this would imply that the pyroclastic beads were degassing at higher
515 fO_2.
516 Hauri et al. (2017) suggested that data below ~20 ppm wt H_2O were dominated by
517 spallogenic H, and suggested magmatic water dominates in lunar samples above this level. This
518 further emphasizes the importance of the "red light/yellow light/green light zones" of water
519 content for D/H interpretation of extraterrestrial materials that we introduced above.
520
521 *2.3.2. Water and D/H of Mare basalts*
522
523 Our knowledge of water and D/H of mare basalts comes primarily from SIMS analyses of
524 two phases: silicate glasses and apatite. These two phases have benefits and pitfalls for inferring
525 hydrogen and D/H values. Apatite is slow to exchange its hydrogen under most conditions
526 (Higashi et al., 2017), thus making it a potentially strong container for preserving lunar water
527 information. Apatite is a common rock-forming phosphate mineral that can contain F, Cl, and
528 OH as essential structural constituents that occupy a single crystallographic site (Pan and Fleet,
529 2002). The relative proportions of F, Cl, and OH in apatite may be used to extract relative
530 fugacity ratios of F, Cl, and OH in the silicate melts or aqueous fluids from which they formed if
531 thermodynamic models are developed for the mixing of F, Cl, and OH components in apatite
532 and for F, Cl, and OH components in multicomponent melt and fluid systems (e.g., Candela
533 1986, Hovis and Harlov 2010). In the absence of such models, the partitioning behavior of F, Cl,

and OH between apatite and melt or fluid can be used to approximate the relative abundances of F, Cl, and OH in fluid and melt systems (e.g., Brenan, 1993, McCubbin et al., 2015b, Boyce et al., 2014, Riker et al. 2018). However, the partitioning cannot be treated with simple Nernst-like partition coefficients given the stoichiometric constraints on F, Cl, and OH abundances in apatite and the lack of constraints on the abundances of F, Cl, and OH in coexisting silicate melts or fluids (Boyce et al., 2014, McCubbin et al., 2015b). This complicates the use of apatite as a quantitative melt hygrometer, especially for mare basalts. Lastly, apatite is a late-crystallizing mineral in lunar magmas, thus only recording information in the last stages of magmatic history.

Glasses record magmatic information directly, without the need for partition coefficients, thus making them ideal for understanding a magma's volatile history, if they do not undergo degassing or water and hydrogen isotope exchange with external reservoirs during cooling. As silicate melts do not cool through the glass transition until they have reached ~2/3 of their liquidus temperatures, magmatic liquids can be susceptible to extensive exchange during cooling. Melts that are trapped in minerals can potentially be armored against further exchange with the magma (Kent, 2008). Yet, even olivine-hosted melt inclusions can undergo substantial H exchange with magmas via diffusive exchange through the crystals, either at magmatic temperatures or during cooling (Gaetani et al., 2012), suggesting that even these records may not be pristine. CO_2 and S can also be affected by this process in olivine-hosted melt inclusions, but F and Cl are not (Bucholz et al., 2013). Furthermore, both apatite and glasses will give poor information on D/H below 50 ppm wt H_2O, due to terrestrial contamination and spallogenic H.

Apatite. Measurements of water contents and/or D/H of apatite in mare basalts have been published by Boyce et al. (2010, 2015), McCubbin et al. (2010a,b), Greenwood et al. (2011), Tartése and Anand (2013), Barnes et al. (2013), Tartése et al. (2013, 2014a,b), and Treiman et al., (2016b). Early studies used apatite to estimate the water content of the Moon, but Boyce et al. (2014) proposed a model for the partitioning of water in apatite, which predicted that OH-rich apatite would only be produced in volatile-poor magmas, due to the strong preference of F over OH or Cl in apatite. This suggests that F-rich, OH-poor apatite would be a better indicator of higher volatile contents in lunar magmas. Thus, while lunar apatite can contain copious amounts of water (over 1 wt.% OH; Tartése et al., 2013), until other evidence of water-rich magmas in lunar samples with OH-rich apatite are found, this mineral should not be used to estimate water contents of lunar magmas or the bulk Moon.

The D/H of apatite in lunar samples is not affected by the model of Boyce et al. (2014), but would be affected by degassing of lunar magmas before the onset of apatite crystallization. Greenwood et al. (2011) found a δD range of -215‰ to 1010‰ in mare basalts, and proposed a cometary source for elevated D/H, and mixing with either solar wind or mantle hydrogen with lower D/H. Tartése and Anand (2013) proposed degassing of H_2 from lunar magmas originally with a δD ~ 100‰ to explain elevated D/H of lunar apatite. They revised this value down to -100‰ for KREEP (K-,Rare Earth Element-,P-rich) samples (Tartése et al., 2014a). KREEP samples have a component of the last 1-2% percent crystallization of the lunar magma ocean (called urKREEP), and are rich in incompatible elements (Warren and Wasson, 1979), and should be volatile-rich. They proposed delivery of chondritic water after the Moon-forming giant impact through crust-breaching impacts, and this idea was further elaborated upon in Barnes et al. (2016).

Pyroclastic glasses and their olivine-hosted melt inclusions. Pyroclastic glasses have been studied by Saal et al. (2008, 2013), Hauri et al. (2011), Füri et al. (2014) and Chen et al. (2015). Saal et al. (2008) suggested that the Moon had primitive material below the magma ocean that was inherited from the Earth. The olivine-hosted melt inclusions studied by Hauri et al. (2011) provided the first direct evidence for magmatic volatile contents above 1000 ppm wt H_2O in the Moon. Saal et al. (2013) found the most water-rich melt inclusions have slightly elevated δD (δD= 270±56‰). Chen et al. (2015) conducted a more extensive study of the volatile contents of pyroclastic glasses and their olivine-hosted melt inclusions, and generally confirmed the results and interpretations of Saal et al. (2008) and Hauri et al. (2011) for the 74220 orange glasses. Importantly, Chen et al. (2015) found high levels of F, Cl, and S in other types of pyroclastic glasses, showing that 74220 is not an anomalous sample, and that the Moon is likely not completely dry (meaning 1 ppm wt H_2O or less). Chen et al. (2015) estimated from H_2O/Ce that the Moon is depleted in water by only a factor of three relative to Earth, similar to the depletion in K for the Moon (Fig. 2) (Warren and Taylor, 2014).

Secondary processes affecting water and D/H of lunar samples. Singer et al. (2017) conducted measurements of H and D/H of olivine-hosted melt inclusions of the slowly cooled samples (12018, 12035, and 12040) of the Apollo 12 olivine basalt suite (Walker et al., 1976). These are very different samples to the pyroclastic glasses that were probably produced by fire-

595 fountain activity on the lunar surface (e.g., McCubbin et al., 2015a). Walker et al. (1976)
596 proposed that the Apollo 12 olivine basalts sampled ~35 m of the basal portion of a magma
597 body, such as a sill, thick lava flow, or lava pond, and that became olivine-rich by gravitationally
598 driven crystal settling. In contrast to the water-rich olivine-hosted melt inclusions of 74220
599 (average δD = 270±56‰), the melt inclusions in Apollo 12 olivine basalts with > 150 ppm wt
600 H_2O were characterized by lower δD values ranging from -183±212‰ to 6±185‰. Diffusion
601 calculations show hydrogen and D/H in the melt inclusions should be exchangeable with external
602 hydrogen reservoirs in these slowly cooled samples (Singer et al., 2017). In agreement with this
603 idea, apatite δD is low (~0‰) in the most slowly cooled sample (12040), while the δD of apatite
604 in the more rapidly cooled 12018 is very high (δD=1439±103‰). This suggests that D/H
605 underwent exchange with a low D/H reservoir during cooling. These results also lend credence
606 to the model proposed by Treiman et al. (2016b) for secondary processes affecting D/H of apatite
607 in slowly cooled mare basalts. Another implication of this study is that olivine-hosted melt
608 inclusions of 74220 (Saal et al., 2013) may have been undergone exchange with solar wind
609 derived hydrogen in near-surface magma chambers (e.g., Gaetani et al., 2012). This suggests
610 caution should be applied when considering hydrogen and D/H in olivine-hosted melt inclusions.

611

612 *2.3.3. Water and D/H of Highlands samples*

613

614 The lunar highlands are the most ancient portions of the lunar surface, and samples of
615 them that have been analyzed have very low water contents and D/H ratios include ferroan
616 anorthosite crust (FAN) and later intrusive rocks (Mg-suite, alkali-suite). Hui et al. (2013) used
617 FTIR to measure 5–6 ppm wt H_2O in plagioclase from FAN, and predicted ~320 ppm wt H_2O for
618 the lunar magma ocean. Hui et al. (2017) measured D/H of this very low water content
619 plagioclase, but these measurements are in the 'red zone' of SIMS analyses and will not be
620 discussed further.

621 Greenwood et al. (2011) found δD = 290±73‰ for apatite with 80 ppm wt H_2O in an
622 alkali anorthosite clast, and suggested this is the value for the hydrogen isotope composition of
623 the lunar mantle. More recent work has found values that overlap with those of mare basalt

apatite (Barnes et al. 2014; Robinson et al., 2016). Measurements of QMD clasts from 15403 and 15404 are much lighter, with apatite in 15404 having a $\delta D = -344 \pm 319‰$ (2σ) and 15403 apatite with $\delta D = -721 \pm 48‰$ (2σ). The extremely light value of apatite in 15403 is anomalous for lunar magmatic samples, but in the expected range of solar wind in the lunar regolith (e.g., Liu et al., 2012).

2.3.4. Isotopes of volatile elements that bear on the question of water and D/H of the Moon

Cl, Zn and K isotopes. Sharp et al. (2010) showed that the Moon had high $\delta^{37}Cl$, unlike other bodies in the Solar System. They suggested that elevated Cl isotope ratios could only be produced in extremely water-poor conditions, and concluded that the Moon had < 1 ppm wt H_2O. The highest $\delta^{37}Cl$ was measured using SIMS in apatite from KREEP basalt 72275. Boyce et al. (2015) studied δD and $\delta^{37}Cl$ of apatite in mare basalts, and found a strong positive correlation of $\delta^{37}Cl$ and Th or La/Lu (both indicators of KREEP signature). They found no correlation between δD and $\delta^{37}Cl$. They argued that the Cl isotopic composition of urKREEP is ~30‰ (the mantle reservoir of KREEP; also the last 1–2% of lunar magma ocean crystallization) and was set during lunar magma ocean outgassing after the loss of water. This would imply that urKREEP is very dry (McCubbin et al., 2015a). Barnes et al. (2016) measured $\delta^{37}Cl$ in apatite from KREEP basalt 15386 and found a positive correlation of $\delta^{37}Cl$ with apatite Cl content. They argued that the lunar magma ocean had a $\delta^{37}Cl$ of ~30‰, and suggested that late crust-breaching impacts could have allowed the urKREEP reservoir to outgas.

The Moon is the only body that currently has resolvable K isotope anomalies (Wang and Jacobsen, 2016). Heavy Zn isotope anomalies have also been measured in lunar materials, which have been interpreted as representing loss of light Zn isotopes during first the proto-lunar disk phase and then during outgassing of the lunar magma ocean (Paniello et al., 2012; Kato et al., 2015). The combination of heavy isotope enrichments for the moderately volatile lithophile element K and the more volatile Zn and Cl argue that the Moon experienced a unique event in the inner Solar System, which is most likely the giant impact event.

652 **N isotopes.** Füri et al. (2015) and Mortimer et al. (2015) measured $\delta^{15}N$ in lunar basalts.
653 Mortimer et al. (2015) measured six lunar basalts and found $\delta^{15}N$=0.35‰, similar to terrestrial
654 atmosphere and earlier measurements of lunar materials (Mortimer et al., 2015 and references
655 therein). Füri et al. (2015) reported a range of $\delta^{15}N$ of -0.2 to 26.7‰, with the higher values
656 similar to some carbonaceous chondrites. They also reported values of $\delta^{15}N < -30$‰, which
657 would be similar to the isotopic composition of Earth's primordial mantle. On the basis of N
658 isotopes, Füri et al. (2015) argued that indigenous lunar volatiles could have been inherited from
659 a proto-lunar disk sourced from the terrestrial mantle or implanted into the lunar mantle during
660 the subsequent late accretion phase.

661

662 *2.3.5. Water abundances of the Moon*

663

664 Geochemical estimates of the water abundance of the Moon primarily come from three
665 datasets: highland samples (Hui et al., 2013, 2017), pyroclastic glasses (Hauri et al., 2015; Chen
666 et al., 2015), KREEP samples (McCubbin et al., 2015a; Greenwood et al., 2017). There are also
667 geophysical and selenogenetic estimates (Karato, 2013; Elkins-Tanton and Grove, 2011,
668 Pahlevan et al. 2016). The range of water abundances for the Moon runs the gamut, from Earth-
669 like levels of 100-300 ppm wt H_2O (Hui et al., 2013; Chen et al., 2015; Hauri et al., 2015;
670 Greenwood et al., 2017), to slightly lower abundances (10-100 wt ppm wt H_2O; Karato, 2013,
671 Pahlevan et al. 2016), to order of magnitude lower abundances of 3-13 ppm wt H_2O (McCubbin
672 et al., 2015a) and < ~10 ppm wt H_2O (Elkins-Tanton and Grove, 2011).

673 **Highland samples.** Hui et al. (2017) used their earlier measurements of water in anorthite from
674 FAN 60015 (Hui et al., 2013) to estimate the water content of the lunar magma ocean to be ~136
675 ppm wt H_2O, without outgassing. If outgassing of H_2 from the magma ocean is called upon to
676 raise the δD of the initial hydrogen reservoir from -250‰ to 300‰ (the lower value is an
677 estimate of the δD of the undegassed magma ocean, and the higher value is similar to values in
678 olivine-hosted melt inclusions in pyroclastic glasses (Saal et al., 2013) and highlands apatite
679 (Greenwood et al., 2011)), estimates of the water content for the initial lunar magma ocean
680 ranges from 1320 to 5000 ppm wt H_2O (Hui et al., 2017).

Pyroclastic glass bead estimates. The pyroclastic glass beads have been used to estimate the water contents of their parent magmas, as well as the whole Moon. Chen et al. (2015) estimated 110 ppm wt H_2O for the mantle source of the pyroclastic glasses. Hauri et al. (2015) estimated that the bulk silicate Moon (BSM) contains 100–300 ppm wt H_2O primarily using the sulfur concentrations and H_2O/Ce of the pyroclastic glass beads.

urKREEP estimates. McCubbin et al. (2015a) postulated that the late residual liquid of the lunar magma ocean would be Cl-enriched relative to H_2O and F, due to magma ocean volatile abundances being controlled by partitioning with anhydrous minerals. They estimated the lunar mantle to have much less water than the Earth, with only 0.15 ppm wt to 5.3 ppm wt H_2O. They predicted that the majority of the Moon's volatiles would be in urKREEP (which they defined as the last 1% residual liquid from magma ocean crystallization). They predicted 300–1250 ppm wt H_2O for urKREEP and 3–13 ppm wt H_2O for the BSM, an order of magnitude less than estimates using pyroclastic glasses (Chen et al., 2015; Hauri et al., 2015).

Greenwood et al. (2017) also predicted that the bulk of the Moon's volatiles would be in the urKREEP from their finding of Cl-rich late-stage glasses in KREEP basalts 15382 and 15386. Due to an order of magnitude depletion in F in lunar samples relative to Earth, they used an H_2O/Ce of 17–30 to estimate lunar water abundances, instead of the higher H_2O/Ce=64 or 77 of orange glasses (Hauri et al., 2015; Chen et al., 2015). They obtained ~1.3 wt.% to 2.4 wt.% H_2O for urKREEP; if urKREEP represents the last 1% of a lunar magma ocean that originated from a 100% molten Moon, then the BSM would contain 130–240 ppm wt H_2O, similar to estimates obtained from the pyroclastic glasses (Hauri et al., 2015). The estimate for urKREEP of Greenwood et al. (2017) is also similar to an estimate for urKREEP of 1.4 wt% H_2O using highlands FAN plagioclase (Hui et al., 2013).

Models for high water content of the Moon. As summarized above, there is a wide range of water content estimates for the Moon. But, the most recent estimates have begun to converge on a water and volatile content for the lunar mantle that is depleted relative to Earth's mantle by an order of magnitude (Greenwood et al., 2017), or less (Chen et al., 2015; Hauri et al., 2015; Hui et al., 2013, 2017).

In contrast, a model of volatile content based on condensation temperature (e.g., Albarède et al., 2015) predicts much higher degrees of depletion. Such a model assumes condensation to

711 solids, but condensation could occur to liquids when pressure of the gas is high. Karato (2013)
712 showed that for condensation to liquid in a high-pressure environment in the Moon-forming disk,
713 the solubility in the liquids is not controlled by the bond strength (e.g., Karato, 2016) and
714 consequently, the degree of depletion of highly volatile elements such as H is much less when
715 condensation occurs to liquids. Similarly, Pahlevan et al. (2016) modeled the behavior of
716 hydrogen during lunar origin process and concluded that proto-lunar disks with terrestrial
717 abundances of hydrogen would dissolve ~10-100 ppm wt H_2O into proto-lunar liquids (see also
718 Canup et al., 2015a,b). Those models are consistent with the K isotope observations suggesting a
719 high-pressure environment in the moon-forming disk (Wang and Jacobsen, 2016).

720

721 *2.3.6. Geophysical constraints on lunar water abundances*

722

723 Although the extensive study of lunar basaltic inclusions by Chen et al. (2015) strongly
724 suggests that the modest degree of depletion in volatile elements such as water (hydrogen) in the
725 lunar mantle is global, it is also important to develop independent methods to constrain the lunar
726 water abundance. To circumvent the ambiguities inherent in geochemical approaches, Karato
727 (2013) used geophysical observations to infer global water content of the lunar interior. Among
728 various geophysical properties, Karato (2013) chose electrical conductivity and tidal Q; both of
729 these properties are controlled by the motion of crystalline defects that depend strongly on water
730 content (for a review on electrical conductivity see Karato and Wang, 2013; for tidal Q, Karato,
731 2013).

732 Electrical conductivity of the Moon was investigated during the Apollo mission using the
733 measurements of time-dependent electromagnetic fields (e.g., Hood et al., 1982; Sonett et
734 al., 1971). In these studies, the depth-variation of electrical conductivity was inferred assuming
735 a one-dimensional model. Tidal deformation occurs on time scales of months-to-years and it
736 involves not only elastic but also viscous deformation. The tidal Q is a measure of the non-elastic
737 part of the deformation. The tidal Q was determined by radar observations of the shape of the
738 Moon (Williams et al., 2001) and is, therefore, known to rather high precision (to within ~10–
739 20%).

Both electrical conductivity and tidal Q depend strongly on the water content and temperature of the body of interest. Consequently, if one uses only one of these observations, then the trade-off between the water content and temperature is strong and the inference of the water content is non-unique. Karato (2013) simultaneously used both properties to more uniquely infer the water content and temperature in the lunar interior. The results show that the lunar interior is cooler (at a depth of 800 km, temperature is ~1350 ± 150 K) than Earth's interior (at a depth of 800 km, temperature is ~2200 ± 100 K), while the water content is similar to, or slightly less than, that of the asthenosphere of Earth (the Moon: 10-100 ppm, Earth: 100 ppm) (Fig. 6). The results support the notion of a not-so-dry Moon inferred from geochemical studies (Saal et al., 2008; Hauri et al., 2011, 2015; Chen et al., 2015).

2.3.7. D/H and sources of the Moon's water

Earth source. Saal et al. (2008) suggested that since the Moon has some water in pyroclastic glasses, parts of the deep Moon may have remained unmelted during the giant impact event. Saal et al. (2013) argue that the elevated D/H of olivine-hosted melt inclusions (δD= 270±56‰) was due to degassing of H_2 from values that were similar to the terrestrial Earth mantle (~-60‰, Clog et al., 2013). This terrestrial signature could also be due to equilibrium dissolution of terrestrial hydrogen in the proto-lunar disk with negligible high-temperature isotopic fractionation (Pahlevan et al. 2016). Robinson et al. (2016) argue that extremely low δD they measured in highland rocks represent a solar-like reservoir in the mantle, and call for parts of the Moon to carry solar-like hydrogen, as has been postulated for reservoirs in the Earth's deep mantle (Hallis et al., 2015).

Carbonaceous chondrite source. The majority of researchers favor a carbonaceous chondrite origin for terrestrial volatiles, due to similarities in δD and $\delta^{15}N$ (e.g., Alexander et al., 2012, 2018; Halliday, 2013; Marty, 2012; Marty et al., 2016). Saal et al. (2013) called for a carbonaceous chondrite origin for lunar water, though they implied that this may also have been a terrestrial relic of the giant impact event. Tartése and Anand (2013) argued for delivery of chondritic impactors to the Moon after the giant impact, and Barnes et al. (2016) developed this

idea further. Füri et al. (2015) argued that N isotopes for the Moon were best matched by carbonaceous chondrites, but with additional identifiable components.

Cometary source. Due to the elevated D/H of most lunar apatites, Greenwood et al. (2011) suggested cometary delivery of water. This would need to occur most likely in the time after the giant impact event and before the lunar crust had undergone significant thickening. Barnes et al. (2016) considered this process for chondritic impactors, but the constraints on the timing of impact delivery are similar for the cometary impactors. An additional constraint on the cometary contribution comes from the dynamical delivery efficiency of outer Solar System bodies to the inner solar system (O'Brien et al., 2018) which suggests that only a small fraction of terrestrial water could be delivered by cometary sources.

2.3.8. Timing of water delivery to the Moon

Pre-Giant Impact. Saal et al. (2008) first suggested that parts of the Moon may have survived the Moon-forming impact relatively unscathed, and still retain their abundances of terrestrial volatiles. Saal et al. (2013) and Hauri et al. (2015) also favored this idea for the majority of the lunar volatiles to have survived the giant impact event.

Giant Impact. Volatile gain and loss accompanying the giant impact would most likely occur during thermal processing in the immediate aftermath of the event. Such post-impact evolution can be separated into two distinct regimes: the proto-lunar disk and magma ocean regimes, the former having received the most attention. Early thinking about the giant impact considered that the proto-lunar disk could have been open with respect to thermal escape of hydrogen (Stevenson, 1987). However, since hydrogen constitutes only a small fraction of the proto-lunar disk, it was subsequently recognized that thermal escape required that the light hydrogen atoms separate from heavier, gravitationally bound silicate vapor species (SiO, O_2) in order to undergo significant escape (Genda, 2004). The process of condensation (Pahlevan and Stevenson, 2008) and molecular diffusion (Nakajima and Stevenson, 2018) were found to be inefficient as means of separating the heavy bound gases from the light unbound hydrogen. Thermal escape of the heavier silicate vapor species requires very distended (>10 Earth radii) disks (Desch and Taylor,

2011), much more distended than found in models of lunar accretion (Salmon and Canup, 2012). Hence, recent thinking on the evolution of the proto-lunar disk considers the proposition that the disk was nearly closed with respect to thermal escape of gases to space (Canup et al., 2015; Charnoz and Michaut, 2015; Hauri et al., 2017; Karato, 2013; Lock et al., 2018; Pahlevan et al., 2016). In these studies, the observed abundances of lunar volatiles are due to liquid-vapor partitioning followed by preferential accretion of the Moon from the liquid fraction. The complementary vapor could, in this setting, be lost to the silicate Earth without violating terrestrial abundance constraints.

A second physical setting that can alter the lunar volatile abundances is the lunar magma ocean, either during a short "naked" magma ocean phase contemporaneous with lunar accretion or after accretion and formation of a flotation crust due to crust-breaching impacts (Barnes et al., 2016). In both cases, the escape of a proto-atmosphere would have been facilitated by the weaker gravity field of the Moon that makes the conditions necessary for hydrodynamic escape easier to achieve. Two lines of evidence for volatile loss from the lunar magma ocean have recently come forward. First, identification of two Cl isotopic reservoirs in the Moon, one associated with a "normal" lunar mantle (δ^{37}Cl~0‰), and the other an isotopically enriched urKREEP end-member (δ^{37}Cl~30‰), suggests ongoing evaporation and fractionation during the formation and closure of these two reservoirs (Boyce et al., 2015), processes that would also have influenced the lunar hydrogen abundances. Secondly, after decades of expended efforts, a K isotopic offset has been observed between the silicate Earth and Moon (Wang and Jacobsen, 2016). This is an important observation because K isotopes do not significantly fractionate during petrologic processes or during liquid-vapor equilibrium and, therefore, constrain the kinetics of volatile loss during an episode that presumably would also have affected lunar hydrogen abundances and isotopic compositions.

Post-Giant Impact. Greenwood et al. (2011) argued for exogeneous delivery of volatiles to the Moon, favoring delivery of cometary water after the giant impact event, and before solidification of a thick lunar crust, likely 10–200 Ma after Moon formation (Elkin-Tanton et al., 2011). Tartése and Anand (2013) suggested a variant on this idea, by calling for delivery of chondritic water via asteroidal delivery. Barnes et al. (2016) undertook detailed modeling of this process and called for a crust-breaching impact to expose the lunar magma ocean and cause it to degas

and fractionate Cl isotopes. The high water contents measured in KREEP materials (e.g., Tartése et al., 2014a) suggest that urKREEP had significant water, as suggested by Greenwood et al. (2017) and Hui et al. (2017), which would likely preclude outgassing under water-poor conditions. Finally, Ustunisik et al. (2015) showed that lunar magmas would degas H before Cl, thus allowing for the possibility of outgassing the magma ocean sequentially, but the dynamics of how that would occur in a crust-breaching impact have yet to be the subject of detailed modeling.

2.4. Mars

2.4.1. Introduction

The cadre of missions to Mars in the last two decades has led to an evolving picture of martian water that argues strongly for the presence of liquid water on the Mars surface in the Noachian and pre-Noachian (~3.7–4.5 Ga) from the presence of fluvial landforms and hydrous minerals (e.g., Carr, 2006; Ehlmann and Edwards, 2014). What is not known is how much water was involved in creating these aqueous environments. Was it global-scale oceans or intermittent wetting with mostly subsurface water? Recent climate models do not require a warm, thick atmosphere to satisfy the current constraints on water availability (e.g., Wordsworth, 2016). During the Hesperian (~3.0–3.7 Ga) there was a change to the current dry atmosphere of Mars, and evaporite deposits mark this transition (Bibring et al., 2006). The current dry climate suggests that surface water has not been an important feature of martian landscape evolution for several billion years. Following orbital and landed observations of ground ice near the poles (Boynton et al., 2002; Smith et al., 2009), large reservoirs of subsurface ice have been found in mid-latitude to near-equatorial regions (Mouginot et al., 2012; Dundas et al., 2018), suggesting that there may be large ice reservoirs on Mars that are not part of the current hydrologic cycle, but could be activated during warming due to martian obliquity cycles. Here we discuss the water abundances and D/H of the three recognized reservoirs for water on Mars: the atmosphere, crust, and mantle.

When Mariner 9 radioed back to Earth the first photographs of Mars obtained from orbit, scientists were disappointed to find a desert-like planet, instead of the potential oasis of life

imagined by the public, due to the early ideas of martian canals promoted by Lowell (1906). The Viking landers in 1976 had mass spectrometers, but only found trace water in the martian atmosphere (Owen, 1992). The Viking mass spectrometers did find elevated levels of ^{15}N (McElroy et al., 1976; Nier et al., 1976), suggesting that there was a loss of an early atmosphere. Owen et al. (1988) measured highly elevated D/H using emission lines of H_2O and HDO. The Viking lander measurements confirmed that the Shergottite-Nakhlite-Chassigny (SNC) meteorite clan were from Mars because trapped gases in impact glasses in the meteorites proved to be almost identical in composition to the current martian atmosphere (Bogard and Johnson, 1983). Watson et al. (1994) first measured D/H in the martian meteorites using SIMS, and found values similar to the martian atmosphere. A review of early measurements of D/H in SNC meteorites can be found in Usui (2018).

2.4.2. Water abundances and D/H of martian reservoirs

Atmospheric water. Current atmospheric water is dominantly sourced from the polar caps, which dominate the recognized surface reservoir of water, and has a total volume of 20–30 mGEL (meters of global equivalent layer) (Kurokawa et al., 2014). The precipitable water column in the present-day atmosphere is < 50 μm (Fisher et al., 2007). The D/H of the present atmospheric water is ~5000‰, but varies on a seasonal basis between ~2000–9000‰ (Fig. 7, Villanueva et al., 2015; Montmessin et al., 2005). The Curiosity rover at Gale Crater using the SAM-TLS also measured δD=4950±1080‰ for the present martian atmosphere, and a much more precise measurement of water from soil components released at 230˚C to 430˚C of δD= 5880±60‰ (Webster et al., 2013). The highest value measured using the SAM-TLS for H_2O was for Rocknest fines during stepped heating of δD = 7010 ± 66‰ (Leshin et al., 2013).

Crustal water. The martian meteorites are samples of the martian crust that have interacted with martian atmospheric water (e.g., Watson et al., 1994). Watson et al. (1994) suggested that the atmospheric water was introduced into the meteorites by alteration of hydrous minerals by later aqueous fluids, possibly during subsolidus cooling. Greenwood et al. (2008) showed from a correlation of zoning of D/H with igneous crystallization of apatite that the D/H was set during the late-stage crystallization of apatite, and that atmospherically-derived water with a high D/H

had mixed with magmatic water of low D/H in the magma, either by assimilation or an igneous hydrothermal system. Hu et al. (2014) showed that an olivine-hosted melt inclusion in GRV 020090 had undergone aqueous alteration by infiltration of high D/H water, suggesting that apatite in martian meteorites needs to be studied more closely with 2-D isotope imaging (isotopography) to better understand how atmospheric waters alter the presumably lower D/H of the magma or protolith.

Ancient water is likely preserved in the oldest known sample of Mars, the ALH 84001 meteorite which underwent an episode of carbonate deposition 3.9-4.1 Ga (Borg et al. 1999). The δD of apatite associated with carbonate can provide an ancient value for D/H of water, if it is not altered by later fluids. One measurement of apatite in ALH 84001 is ~3000‰; measurement of δD in associated carbonate reach maximum δD ~ 2000‰ (Sugiura and Hoshino, 2000; Boctor et al., 2003), suggesting that water on the martian surface was as low as 2000–3000‰ at 3.9-4.1 Ga.

The NWA 7034 martian meteorite ("Black Beauty") is a breccia and is the second sample of old martian crust in our collections. The rock has a bulk age of ~ 2 Ga (Agee et al., 2013), but igneous clasts in the meteorite record ancient ages of ~4.44 Ga (Nyquist et al., 2016), confirming the early separation of the mantle and crustal reservoirs on Mars. The clasts and matrix of the breccia also host martian water measured during stepped heating and mass spectrometry for δD and oxygen isotopes (Agee et al., 2013). The main martian water-bearing phases in the meteorite are a mélange of hydrous Fe-oxide phases, which suggest the importance of these phases for hosting water in the martian crust (Muttik et al., 2014). Evidence for fluid-rock interactions in the martian crust have also been found from phosphate minerals in NWA 7034 (Liu et al., 2016). The wide range of ages obtained for NWA 7034 require that apatite D/H measurements come from clasts that can be dated, in order to assess the D/H of martian crustal water in different epochs (e.g., Greenwood et al., 2008; Villanueva et al., 2015).

A third distinct reservoir of crustal water on Mars has been suggested from water trapped in impact glasses of martian meteorites that were excavated from the martian crust (Usui et al., 2015). Usui et al. (2015) proposed that there is a reservoir in the martian crust with a δD ~1000–2000‰ that is sampled by the impact glasses, and is similar to Hesperian clays measured by the Curiosity rover using the SAM-TLS (δD=2000±200‰) (Mahaffey et al., 2015). This intermediate D/H water reservoir (to distinguish it from the low primordial D/H of the mantle

(see below) and the more D-enriched atmospheric water) could be ice or hydrated crustal minerals that have been isolated from exchange with the atmospheric water and represents ancient water, similar to that which deposited the Hesperian-aged clays measured by Curiosity rover. The existence of this putative reservoir in the impact glasses of martian meteorites has been called into question, as Hallis (2017) argue that low water-containing glasses in martian meteorites have likely been affected by shock implantation of the martian atmosphere during the shock event that liberated the samples from the martian crust. It remains to be seen if this reservoir exists in martian meteorites, but the reservoir does exist in Hesperian-aged clays on the martian surface (Mahaffey et al., 2015).

Mantle water. Mars is thought to have had a different early history to that of the Earth, and would have started as a planetary embryo and then underwent early igneous differentiation during a magma ocean phase (Elkins-Tanton et al. 2005). It is generally believed that the crust and mantle did not undergo recycling or melting events that would later significantly mix mantle and crustal components (e.g., Brandon et al., 2000; Debaille et al., 2007; Foley et al., 2005; Kleine et al., 2009), suggesting that mantle water may represent a very early episode of volatile acquisition by Mars (Brasser, 2013).

Usui et al. (2012) estimated the primordial mantle water to have $\delta D < 275‰$ from SIMS measurements of water in olivine-hosted melt inclusions of Yamato (Y-) 980459. This meteorite is believed to represent an early melt from a geochemically depleted source in the martian mantle, and its melt inclusions are interpreted to represent undegassed mantle water. Other estimates of the δD of the martian mantle are 900‰ from apatite in QUE 94201 (Leshin, 2000), and -100‰ from apatite in Nakhla (Hallis et al., 2012). This may indicate significant mantle heterogeneity, or terrestrial contamination during analysis of apatite (e.g., Greenwood et al., 2008; Boctor et al., 2003). As discussed earlier, all H isotope measurements of martian meteorites are challenging, due to the prevalence of fractures which are the result of high shock pressures experienced by these rocks as they left Mars (Figure 6).

Water abundances for the martian mantle of 73–290 ppm wt H_2O have been estimated from apatite in both geochemically enriched and depleted shergottites (McCubbin et al., 2012b) using experimentally determined partition coefficients for water and apatite in shergottite magmas (McCubbin et al., 2015b). Due to the early formation of Mars, and the lack of crustal

recycling, water in the mantle is likely to be primordial, and not delivered by later additions of chondrites or comets. This suggests significant reservoirs for primordial H in the martian interior (McCubbin et al. 2012b).

2.4.3. Evolution of water through time on Mars

Based on the low δD of water in apatite from the ancient ALH 84001 meteorite, it was argued that Mars suffered a two-stage loss of water: significant early loss of water up to 3.9-4.1 Ga, followed by only modest loss since (Greenwood et al., 2008). This significant early loss of water would likely be due to hydrodynamic escape (Hunten et al., 1987). Using the mantle estimate of Usui et al. (2012) for D/H of primordial water, Kurokawa et al. (2014) modeled the loss of water due to atmospheric escape as a two-stage process. Their model suggested loss of >41–99 mGEL before 4 Ga, and a lower loss rate of >10–53 mGEL since then. Usui (2018) reports that an updated version of the model of Kurokawa et al. (2014) with atmospheric D/H of 7000‰ (Leshin et al., 2013; Villanueva et al., 2015) suggests ~40% higher loss of water. Regardless, these estimates are much lower than amounts of water loss based on geomorphology of ~100–1000 mGEL (Carr and Head, 2003; Di Achille and Hynek, 2010; Head et al., 1999; Ormö et al., 2004). If Mars had oceans, then a great deal of water is missing and could be buried water ice (Clifford and Parker, 2001; Grimm et al. 2017). Usui et al. (2015) predict that this ice would have δD of ~1000–2000‰.

2.4.4. Timing of water delivery and sources of water to Mars

Crust. The lack of viable crustal recycling mechanisms on Mars, combined with its early accretion and early magma ocean crystallization, suggests that the ancient crust of Mars (the Noachian-aged southern highlands) holds the outgassed inventories of volatile elements unable to escape from the atmosphere (e.g., S and Cl). The likely early crystallization of the magma ocean would suggest that the Noachian highlands would have witnessed later delivery of volatiles from chondritic or cometary material, as well as volatile-bearing material during the late

heavy bombardment. This suggests that early martian crustal water may reflect these sources of water.

Mantle. There are four estimates for the H isotopic composition of the martian mantle. Usui et al. (2012) estimate the martian mantle δD <275‰, as they argue that water in the olivine-hosted melt inclusion they measured in Y-980459 may have been affected by early primordial degassing that would have led to elevated D/H. The early formation of Mars and lack of crustal recycling argue that martian mantle water may preserve one of the earliest records of accretion of volatiles in the Solar System. A δD of 275‰ is not similar to any classes of carbonaceous chondrites, as this is heavier than CI, CM, and CV chondrites, but lighter than CR and Tagish Lake (Alexander et al., 2012; 2018 in the same special volume), suggesting that a chondritic origin for martian water requires multiple components.

Three other values for the martian mantle come from apatite in the depleted shergottite QUE 94201 (δD=900±250‰; Leshin, 2000), the fall Nakhla (δD=-111±62‰; Hallis et al., 2012), and the recent fall Tissint (δD=116±94‰) (Mane et al., 2016). If these values are representative of the martian mantle, and are not a result of terrestrial contamination causing significant lowering of D/H (e.g., Greenwood et al., 2008; Boctor et al., 2003), then this would suggest the martian mantle is quite heterogeneous and poorly mixed. If the martian mantle δD ranges from -100‰ to 900‰, this would be similar to the range of D/H expected for a mixture of chondritic and cometary material, and also similar to the D/H of asteroidal water (δD: -400‰ to 1300‰; Yurimoto et al., 2014).

2.4.5. Geophysical constraints on water in the martian mantle

Similar to the Moon, the tidal dissipation of Mars is well constrained from the analysis of the motion of its satellites Phobos and Deimos (Lainey et al., 2007). Electrical conductivity of martian interior was also estimated from electromagnetic field observations (Civet and Tarits, 2014). Consequently, one can use these results to infer temperature and water content in Mars similar to the case on the Moon (Karato, 2013).

Relatively small tidal Q (80 +/- 0.7) (i.e., high degree of energy loss) and high conductivity (~1 S/m at 1000 km depth) suggest the relatively "wet" interior of Mars. In contrast

1011 to this expectation, using the laboratory data on electrical conductivity by (Yoshino et al., 2012),
1012 (Verhoeven and Vasher, 2016) argued that the electrical conductivity of the martian mantle can
1013 be explained by the high FeO content without invoking water. Note, however that (Yoshino et
1014 al., 2012) did not measure the water content in their samples, and their results on the influence of
1015 FeO on electrical conductivity of olivine at high pressure are in marked contrast to the well-
1016 established results on the influence of FeO on electrical conductivity at room pressure. Since the
1017 influence of pressure on electrical conductivity is small (Dai and Karato, 2014a; Xu et al., 2000),
1018 this large difference is likely due to the high water content in their samples (Karato, 2017).
1019 Indeed, by measuring the electrical conductivity as a function of both water content and FeO
1020 content, (Dai and Karato, 2014b) showed that the influence of FeO on electrical conductivity in
1021 olivine is much smaller than that reported by (Yoshino et al., 2012). If one uses the results by
1022 (Dai and Karato, 2014b), one would conclude that a substantial amount of water is present in the
1023 martian mantle. However, there have been no detailed studies on the water content in Mars using
1024 geophysical observations.

1025

1026 **3. Summary**

1027

1028 The abundances of water and other volatiles in the silicate mantles of the inner Solar
1029 System bodies are not well constrained at this time. The detection of Cl-bearing lava flows, as
1030 well as evidence for C and S, show that even Mercury has more volatiles than might be expected
1031 from volatile-poor precursor materials that are predicted this close to the Sun (e.g., Albaréde,
1032 2009). Abundances for water in the mercurian mantle are expected to be low, due to the highly
1033 reducing nature of Mercury (e.g., Hirschmann et al., 2012). Venus has Earth-like levels of C and
1034 N in its atmosphere, suggesting Venus may have accreted Earth-like levels of water, having lost
1035 the bulk of it during the magma ocean (Hamano et al. 2013) or water ocean (Ingersoll, 1969,
1036 Kasting and Pollack, 1983) phases, with some small fraction still extant in the mantle (Elkins-
1037 Tanton et al., 2007). The low abundance of high D/H water in the venusian atmosphere strongly
1038 suggest that significant amounts of water have been lost to space over time.
1039 The interior water budget of the Moon is highly controversial and a wide range of values
1040 have been estimated. Volatile/refractory element ratios of olivine-hosted melt inclusions (Chen et
1041 al., 2015; Hauri et al., 2015; 2017) and KREEP basalt (Greenwood et al., 2017) are in agreement

1042 with estimates from H_2O in plagioclase from ferroan anorthosite (Hui et al., 2013), which all
1043 suggest ~100-300 ppm wt H_2O for the lunar interior. This range is very similar to that postulated
1044 for the Earth's upper mantle (e.g., Peslier et al., 2017). These high, Earth-like values are in
1045 contrast to geophysical and selenogenetic studies which suggest 10-100 ppm wt H_2O for the
1046 lunar interior (Karato, 2013; Pahlevan et al., 2016). Much lower abundances of water for the
1047 lunar interior are suggested from Cl isotopes of lunar materials (Sharp et al., 2010) and magma
1048 ocean modeling studies which argue for ~ < 10 ppm wt H_2O.
1049 The amount of water on Mars has been a controversial subject for decades (Carr, 2006).
1050 Current estimates suggest the martian mantle contains 73-290 ppm wt H_2O (McCubbin et al.,
1051 2012b), which is similar to estimates for Earth's upper mantle. This amount of water would
1052 argue that the martian interior can be a significant source of water and could have supported an
1053 early, active hydrosphere on Mars.
1054 The inner Solar System is believed to have been volatile-depleted at the time of terrestrial
1055 planet formation (Albaréde, 2009; Dauphas and Morbidelli, 2014). Mechanisms for the timing
1056 and delivery of water and other volatiles to the inner Solar System are reviewed in the chapter in
1057 this volume by O'Brien et al. (2018). The currently favored mechanism involves gravitational
1058 scattering of carbonaceous chondrite planetesimals from ~ > 3 AU into the inner Solar System
1059 and their accretion during the latter parts of the Earth's growth, but before the end of the Earth's
1060 core formation (Walsh et al., 2011; O'Brien et al., 2018), since they can be scattered inwards
1061 very early, but due to their eccentric orbits, they might not hit the Earth until relatively late in its
1062 growth. Spectral similarities between volatile-rich C-type asteroids and carbonaceous chondrites
1063 support this theory (e.g., Morbidelli et al., 2012). Carbonaceous chondrites are also favored
1064 sources of water for the inner Solar System, due to similarities in volatile isotope and element
1065 ratios (e.g., Alexander et al., 2012, 2018; Halliday, 2013; Marty, 2012; Marty et al., 2016).
1066 Carbonaeous chondrites have also been suggested as the source of water for differentiated
1067 meteorites, such as the parent bodies of the eucrites and angrites (Sarafian et al., 2014, 2017).
1068 The angrites and eucrites record melting events within ~1-2 Ma of the formation of CAIs, and
1069 are thus younger than the carbonaceous chondrite parent bodies (e.g., Alexander et al., 2018).
1070 The differentiated meteorites require that at least some water and volatiles were delivered inside
1071 the orbit of Jupiter within 2 Ma of CAI formation, and before the formation of carbonaceous
1072 chondrite parent bodies.

Enstatite chondrites or material like the EC's has been suggested to be an important component of the Earth's building blocks (Wänke and Dreibus, 1988; Rubie et al. 2011), and could be an important component for Mars (Dreibus and Wänke, 1985, Sanloup et al. 1999) and the other inner Solar System bodies. The water abundance of the enstatite chondrites is not well known due to the confounding influence of terrestrial weathering (Jarosewich et al., 1990) but EC's have abundant C and N (Fig. 3; Grady et al., 1986), suggesting that the material in the terrestrial planet forming regions may not have been as volatile-poor as is currently advocated (e.g., Albaréde, 2009; Dauphas and Morbidelli, 2014).

Acknowledgements—We thank the organizing committee for inviting us to write this chapter. JPG also thanks K. Abe for assistance with figure preparation, M. Gilmore for discussions regarding Venus, and S. Itoh, N. Sakamoto and H. Yurimoto for discussions of water measurements using SIMS and for discussions on volatile delivery mechanisms to the Solar System. This work was supported by NASA-LASER (NNX14AQ76G) and NASA-EW (NNX17AE26G) to JPG, and by JSPS (16H04073, 15KK0153, 17H06459) to TU.

References

C.B. Agee, N.V. Wilson, F.M. McCubbin, K. Ziegler, V.J. Polyak, Z.D. Sharp, Y. Asmerom, M.H. Numm, R. Shaheen, M.H. Thiemens, A. Steele, M.L. Fogel, R. Bowden, M. Glamoclija, Z. Zhang, S.M. Elardo, Unique meteorite from Early Amazonian Mars: Water-rich basaltic breccia Northwest Africa 7034. Sciencexpress doi:10.1126/science.1228858 (2013)

F. Albarède, Volatile accretion history of the terrestrial planets and dynamic implications. Nature **461**, 1227–1233 (2009)

F. Albarède, E. Albalat, C.-T.A. Lee, An intrinsic volatility scale relevant to the Earth and Moon and the status of water in the Moon. Meteor. Planet. Sci. **50**, 568–577. (2015)

C.M.O.'D. Alexander, K.D. McKeegan, K. Altwegg, Water reservoirs in small planetary bodies: meteorites, asteroids, and comets. Space Sci. Rev. 214, (this book) 36 (2018) https://doi.org/10.1007/s11214-018-0474-9

C.M.O.'D. Alexander, R. Bowden, M.L. Fogel, K.T. Howard, C.D.K. Herd, L.R. Nittler, The provenances of asteroids, and their contributions to the volatile inventories of the terrestrial planets. Science **337**, 721,(2012) https://doi.org/10.1126/science.1223474

J.J. Barnes, D.A. Kring, R. Tartèse, I.A. Franchi, M. Anand, S.S. Russell, An asteroidal origin for water in the Moon. Nat. Commun. **7**, 11684 (2016)

J.J. Barnes, R. Tartèse, M. Anand, F.M. McCubbin, I.A. Franchi, N.A. Starkey, S.S. Russell, The origin of water in the primitive Moon as revealed by the lunar highlands samples. Earth Planet. Sci. Lett. **390**, 244–252 (2014)

J.J. Barnes, I.A. Franchi, M. Anand, R. Tartèse, N.A. Starkey, M. Koike, Y. Sano, and S.S. Russell, Accurate and precise measurements of the D/H ratio and hydroxyl content in lunar apatites using NanoSIMS. Chem. Geol. **337,** 48-55 (2013)

Basaltic Volcanism Study Project *Basaltic Volcanism on the Terrestrial Planets*, New York: Pergamon Press. 1286 pp (1981)

W. Benz, W.L. Slattery, A.G.W. Cameron, Collisional stripping of Mercury's mantle. Icarus **74,** 516-528 (1988)

J.P. Bibring, Y. Langevin, J.F. Mustard, F. Poulet, R. Arvidson, A. Gendrin, B. Gondet, N. Mangold, P. Pinet, F. Forget, M. Berthé, C. Gomez, D. Jouglet, A. Soufflot, M. Vincendon, M. Combes, P. Drossart, T. Encrenaz, T. Fouchet, R. Merchiorri, G. Belluci, F. Altieri, V. Formisano, F. Capaccioni, P. Cerroni, A. Coradini, S. Fonti, O. Korablev, V. Kottsov, N. Ignatiev, V. Moroz, D. Titov, L. Zasova, D. Loiseau, N. Mangold, P. Pinet, S. Douté, B. Schmitt, C. Sotin, E. Hauber, H. Hoffmann, R. Jaumann, U. Keller, T. Duxbury, G. Neukum, Global mineralogical and aqueous Mars history derived from OMEGA/Mars Express data. Science **312,** 400-404 (2006)

T.A. Bida, R.M. Killen, T.H. Morgan, Discovery of calcium in Mercury's atmosphere. Nature **404**, 159–161 (2000)

D.T. Blewett, M.S. Robinson, B.W. Denevi, J.J. Gillis-Davis, J.W. Head, S.C. Solomon, G.M. Holsclaw, W.E. McClintock, Multispectral images of Mercury from the first MESSENGER flyby: Analysis of global and regional color trends. Earth Planet. Sci. Lett. **285,** 272-282 (2009)

N.Z. Boctor, C.M.O'D. Alexander, J. Wang, E. Hauri, The sources of water in Martian meteorites: Clues from hydrogen isotopes. Geochim. Cosmochim. Acta **67,** 3971-3989 (2003)

D.D. Bogard, P. Johnson, Martian gases in an Antarctic meteorite? Science **221,** 651-654 (1983)

1135 L.E. Borg, J.N. Connelly, L.E. Nyquist, C.Y. Shih, H. Wiesmann, Y. Reese, The age of the
1136 carbonates in martian meteorite ALH84001 Science **286,** 90-94 (1999)
1137 J.W. Boyce, S.M. Tomlinson, F.M. McCubbin, J.P. Greenwood, A.H. Treiman, The Lunar Apatite
1138 Paradox. Science **344,** 400-402 (2014)
1139 J.W. Boyce, Y. Liu, G.R. Rossman, Y. Guan, J.M. Eiler, E.M. Stolper, L.A. Taylor, Lunar apatite
1140 with terrestrial volatile abundances. *Nature* **466**, 466-470 (2010)
1141 J.W. Boyce, A.H. Treiman, Y. Guan, C. Ma, J.M. Eiler, J. Gross, J.P. Greenwood, E.M. Stolper,
1142 The chlorine isotope fingerprint of the lunar magma ocean. Science Adv. **1,** e1500380 (2015)
1143 W. V. Boynton, W. C. Feldman, S. W. Squyres, T. H. Prettyman, J. Brückner, L. G. Evans, R. C.
1144 Reedy, R. Starr, J. R. Arnold, D. M. Drake, P. A. J. Englert, A. E. Metzger, Igor Mitrofanov,
1145 J. I. Trombka, C. d'Uston, H. Wänke, O. Gasnault, D. K. Hamara, D. M. Janes, R. L. Marcialis,
1146 S. Maurice, I. Mikheeva, G. J. Taylor, R. Tokar, C. Shinohara, Distribution of Hydrogen in the
1147 Near Surface of Mars: Evidence for Subsurface Ice Deposits. Science **297,** 81-85. (2002) DOI:
1148 10.1126/science.1073722
1149 A.D. Brandon, R.J. Walker, J.W. Morgan, G.G. Goles, Re-Os isotopic evidence for early
1150 differentiation of the Martian mantle. Geochim. Cosmochim. Acta **64,** 4083-4095 (2000)
1151 R. Brasser, The formation of Mars: Building blocks and accretion time scale. Space Sci. Rev. **174,**
1152 11-25 (2013)
1153 J.M. Brenan, Partitioning of fluorine and chlorine between apatite and aqueous fluids at high-
1154 pressure and temperature - Implications for the F and Cl content of high P-T fluids. Earth
1155 Planet. Sci. Lett. **117,** 251-263 (1993)
1156 A.L. Broadfoot, D.E. Shemansky, S. Kumar, Mariner 10: Mercury atmosphere. Geophys. Res.
1157 Lett. **3**, 577– 580 (1976)
1158 A.L. Broadfoot, S. Kumar, M.J.S. Belton, Mercury's atmosphere from Mariner 10: Preliminary
1159 results. Science **185**, 166–169 (1974)
1160 S.M. Brown, L.T. Elkins-Tanton, Compositions of Mercury's earliest crust from magma ocean
1161 models. Earth Planet. Sci. Lett. **286,** 446-455 (2009)
1162 C.E. Bucholz, G.A. Gaetani, M.D. Behn, N. Shimizu, Post-entrapment modification of volatiles
1163 and oxygen fugacity in olivine-hosted melt inclusions. Earth Planet. Sci. Lett. **374,** 145-155
1164 (2013)

P.A. Candela, Toward a thermodynamic model for the halogens in magmatic systems - an application to melt vapor apatite equilibria. Chem. Geol. **57,** 289-301 (1986)

R. Canup, C. Visscher, J. Salmon, B. Fegley, Protolunar disk evolution and the depletion of volatile elements in the Moon, Lunar Planet. Sci. Conf. **XLVI,** abstract #2304 (2015a)

R. Canup, C. Visscher, J. Salmon, B. Fegley, Lunar volatile depletion due to incomplete accretion within an impact-generated disk, Nature Geosci. **8,** 918-921 (2015b).

M.H. Carr, *The surface of Mars*. Cambridge University Press, Cambridge, UK. 322 pp. (2006)

M.H. Carr, J.W. Head, Oceans on Mars: An assessment of the observational evidence and possible fate. J. Geophys. Res. **108,** doi: 10.1029/2002JE001963 (2003)

N.L. Chabot, E.A. Wollack, R.L. Klima, M.E. Minitti, Experimental constraints on Mercury's core composition. Earth Planet. Sci. Lett. **390,** 199-208 (2014a)

N.L. Chabot, C.M. Ernst, B.W. Denevi, H. Nair, A.N. Deutsch, D.T. Blewett, S.L. Murchie, G.A. Neumann, E. Mazarico, D.A. Paige, J.K. Harmon, J.W. Head, S.C. Solomon, Images of surface volatiles in Mercury's polar craters acquired by the MESSENGER spacecraft. Geology **42,** 1051-1054 (2014b)

S. Charnoz, C. Michaut, Evolution of the protolunar disk: Dynamics, cooling timescale and implantation of volatiles onto the Earth. Icarus 260, 440-463 (2015)

Y. Chen, Y. Zhang, Y. Liu, Y. Guan, J. Eiler, E.M. Stolper, Water, fluorine, and sulfur concentrations in the lunar mantle. Earth Planet. Sci. Lett. **427,** 37-46 (2015)

F. Civet, P. Tarits, Electrical conductivity of the mantle of Mars from MGS magnetic observations. Earth, Planets, Space **66,** 66-85 (2014)

S.M. Clifford, T.J. Parker, The evolution of the Martian hydrosphere: Implications for the fate of a primordial ocean and the current state of the northern plains. Icarus **154,** 40-79 (2001)

M. Clog, C. Aubaud, P. Cartigny, L. Dosso, The hydrogen isotopic composition and water content of southern Pacific MORB: a reassessment of the D/H ratio of the depleted mantle reservoir. Earth Planet. Sci. Lett. **381**, 156–165 (2013)

L. Dai, S. Karato, The effect of pressure on hydrogen-assisted electrical conductivity of olivine. Phys. Earth Planet. Int. **232,** 51-56 (2014a)

L. Dai, S. Karato, The influence of FeO and H content on the electrical conductivity of olivine: Applications to terrestrial planets with different FeO content. Earth Planet. Sci. Lett. **237,** 73-79 (2014b)

1196 N. Dauphas, A. Morbidelli, Geochemical and planetary dynamical views on the origin of Earth's
1197 atmosphere and oceans, in *Treatise on Geochemistry*, ed. by A.S. Davis 2nd ed. (Elsevier,
1198 Amsterdam), pp. 1–35 (2014)
1199 V. Debaille, A.D. Brandon, Q.Z. Yin, B. Jacobsen, Coupled 142Nd–143Nd evidence for a
1200 protracted magma ocean in Mars. Nature **450,** 525–528 (2007)
1201 S.J. Desch, G.J. Taylor, A model of the Moon's volatile depletion. Lunar Plan. Sci. Conf., **XLII,**
1202 abstract#2005 (2011)
1203 G. Di Achille, B.M. Hynek, Ancient ocean on Mars supported by global distribution of deltas and
1204 valleys. Nature Geosci. **3,** 459-463 (2010)
1205 T.M. Donahue, J.H. Hoffman, R.R. Hodges, A.J. Watson, Venus was wet—a measurement of the
1206 ratio of deuterium to hydrogen. Science **216**, 630–633, (1982)
1207 G. Dreibus, H. Wänke, Mars, a volatile-rich planet. Meteoritics **20,** 367–381 (1985)
1208 C.M. Dundas, A.M. Bramson, L. Ojha, J.J. Wray, M.T. Mellon, S. Byrne, A.S. McEwen, N.
1209 Putzig, D. Viola, S. Sutton, E. Clark, J. W. Holt, Exposed subsurface ice sheets in the Martian
1210 mid-latitudes. Science **359,** 199-201 (2018)
1211 D.S. Ebel, R.O. Sack, Djerfisherite: nebular source of refractory potassium. Contr. Mineral. Petrol.
1212 **166,** 923-934 (2013)
1213 B.L. Ehlmann, C.S. Edwards, Mineralogy of the Martian surface. Ann. Rev. Earth Planet. Sci.**42,**
1214 291-315 (2014)
1215 L.T. Elkins-Tanton, T.L. Grove, Water (hydrogen) in the lunar mantle: results from petrology and
1216 magma ocean modeling. Earth Planet. Sci. Lett. **307**, 173–179 (2011)
1217 L.T. Elkins-Tanton, S.E. Smrekar, P.C. Hess, E.M. Parmentier, Volcanism and volatile recycling
1218 on a one-plate planet: Applications to Venus. J. Geophys. Res. **112**, E04S06 (2007)
1219 L.T. Elkins-Tanton, P.C. Hess, E.M. Parmentier, Possible formation of ancient crust on Mars
1220 through magma ocean processes. J. Geophys. Res. **110,** E12S01, doi:10.1029/2005JE002480
1221 (2005)
1222 L.G. Evans, P.N. Peplowski, F.M. McCubbin, T.J. McCoy, L.R. Nittler, M.Y. Zolotov, D.S. Ebel,
1223 D.J. Lawrence, R.D. Starr, S.Z. Weider, S.C. Solomon, Chlorine on the surface of Mercury:
1224 MESSENGER Gamma-Ray measurements and implications for the planet's formation and
1225 evolution. Icarus **257,** 417-427 (2015)

L.G. Evans, P.N. Peplowski, E.A. Rhodes, D.J. Lawrence, T.J. McCoy, L.R. Nittler, S.C. Solomon, A.L. Sprague, K.R. Stockstill-Cahill, R.D. Starr, S.Z. Weider, W.V. Boynton, D.K. Hamara, J.O. Goldsten, Major-element abundances on the surface of Mercury: Results from the MESSENGER Gamma-Ray Spectrometer. J. Geophys. Res. **117,** E00L07 (2012)

B. Fegley, Jr., Venus, in *Meteorites, Comets, and Planets*, (Ed. A.M. Davis), in *Treatise on Geochemistry 2nd ed.*, Elsevier-Pergamon, Oxford, pp. 127-146, (2014) doi:10.1016/B978-0-08-095975-7.00122-4

D.A. Fisher, Mars' water isotope (D/H) history in the strata of the North Polar Cap: Inferences about the water cycle. Icarus **187,** 430-441 (2007)

C.N. Foley, M. Madhwa, L.E. Borg, P.E. Janney, R. Hines, T.L. Grove, The early differentiation history of Mars from 182W–142Nd isotope systematics in the SNC meteorites. Geochim. Cosmochim. Acta **69,** 4557–4571 (2005)

I. Friedman, J.R. O'Neil, J.D. Gleason, K. Hardcastle, The carbon and hydrogen content and isotopic composition of some Apollo 12 materials. Proc. Lunar Sci. Conf. **2,** 1407-1415 (1971)

E. Füri, E. Deloule, New constraints on the production rate of cosmogenic deuterium at the moon's surface. Lunar Planet. Sci. Conf. **47,** abstract #1351 (2016)

E. Füri, P.H. Barry, L.A. Taylor, B. Marty, Indigenous nitrogen in the Moon: constraints from coupled nitrogen–noble gas analyses of mare basalts. Earth Planet. Sci. Lett. **431**, 195–205 (2015)

E. Füri, E. Deloule, A.A. Gurenko, B. Marty, New evidence for chondritic lunar water from combined D/H and noble gas analyses of single Apollo 17 volcanic glasses. Icarus **229**, 109–120 (2014)

G.A. Gaetani, J.A. O'Leary, N. Shimizu, C.E. Bucholz, and M. Newville, Rapid re-equilibration of H_2O and oxygen fugacity in olivine-hosted melt inclusions. Geology **40**, 915–918. (2012)

H. Genda, M. Ikoma, Origin of the ocean on the Earth: early evolution of water D/H in a hydrogen-rich atmosphere. Icarus **194**, 42–52, https://doi.org/10.1016/j.icarus.2007.09.007 (2008)

H. Genda, Effects of Giant Impacts on the Atmosphere Formation of Terrestrial Planets. University of Tokyo, Tokyo (2004)

M. Gilmore, A. Treiman, J. Helbert, S. Smrekar, Venus surface composition constrained by observation and experiment. Space Sci. Rev. **212**(3–4), 1511–1540 (2017) https://doi.org/10.1007/ s11214-017-0370-8

1257 T.A. Goudge, J.W. Head, L. Kerber, D.T. Blewett, B.W. Denevi, D.L. Domingue, J.J. Gillis-Davis,
1258 K. Gwinner, J. Helbert, G.M. Holsclaw, N.R. Izenberg, R.L. Klima, W.E. McClintock, S.L.
1259 Murchie, G.A. Neumann, D.E. Smith, R.G. Strom, Z. Xiao, M.T. Zuber, S.C. Solomon, Global
1260 inventory and characterization of pyroclastic deposits on Mercury: New insights into
1261 pyroclastic activity from MESSENGER orbital data. J. Geophys. Res. **119,** 635-658 (2014)
1262 M.M. Grady, I.P. Wright, L.P. Carr, C.T. Pillinger, Compositional differences in enstatite
1263 chondrites based on carbon and nitrogen stable isotope measurements. Geochim. Cosmochim.
1264 Acta **50,** 2799-2813 (1986)
1265 J.P. Greenwood, N. Sakamoto, S. Itoh, P.H. Warren, J.A. Singer, K. Yanai, H. Yurimoto, The
1266 lunar magma ocean volatile signature recorded in chlorine-rich glasses in KREEP basalts
1267 15382 and 15386. Geochem. J. **51,** 105-114 (2017)
1268 J.P. Greenwood, S. Itoh, N. Sakamoto, P.H. Warren, L.A. Taylor, and H. Yurimoto, Hydrogen
1269 isotope ratios in lunar rocks indicate delivery of cometary water to the Moon. Nat. Geosci. **4**,
1270 79-82 (2011)
1271 J.P. Greenwood, S. Itoh, N. Sakamoto, E. Vicenzi, H. Yurimoto, Hydrogen isotope evidence for
1272 loss of water from Mars through time. Geophys. Res. Lett. **35,** L05203,
1273 doi:10.1029/2007GL032721 (2008)
1274 R.E. Grimm, K.P. Harrison, D.E. Stillman, M.R. Kirchoff, On the secular retention of ground
1275 water and ice on Mars, J. Geophys. Res. Planets, **122,** 94–109, doi:10.1002/2016JE005132.
1276 (2017)
1277 D.H. Grinspoon, Implications of the high deuterium-to-hydrogen ratio for the sources of water in
1278 Venus' atmosphere, Nature **363**, 428-431 (1993)
1279 D.H. Grinspoon, J.S. Lewis, Cometary water on Venus: Implications of stochastic impacts. Icarus
1280 **74,** 21-35 (1988)
1281 K.P. Jochum, N.T. Arndt, A.W. Hofmann, Nb-Th-La in komatiites and basalts: constraints on
1282 komatiite petrogenesis and mantle evolution. Earth Planet. Sci. Lett. **107**, 272–289 (1991)
1283 A.N. Halliday, The origins of volatiles in the terrestrial planets. Geochim. Cosmochim. Acta **105**,
1284 146–171 (2013)
1285 A.N. Halliday, D. Lee, S. Tommasini, G.R. Davies, C.R. Paslick, J.G. Fitton, D.E. James,
1286 Incompatible trace elements in OIB and MORB and source enrichment in the sub-oceanic
1287 mantle. Earth Planet. Sci. Lett. **133**, 379–395 (1995)

1288 L.J. Hallis, D/H ratios of the inner solar system. Phil. Trans. R. Soc. A **375**, 20150390 (2017)
1289 L.J. Hallis, G.R. Huss, K. Nagashima, G.J. Taylor, S.A. Halldórsson, D.R. Hilton, M.J. Mottl, K.J.
1290 Meech, Evidence for primordial water in Earth's deep mantle. Science **350**, 795–797,
1291 https://doi.org/ 10.1126/science.aac4834 (2015)
1292 L.J. Hallis, G.J. Taylor, K. Nagashima, G.R. Huss, Magmatic water in the martian meteorite
1293 Nakhla. Earth Plan. Sci. Lett. **359-360**, 84-92 (2012)
1294 K. Hamano, Y. Abe, H. Genda, Emergence of two types of terrestrial planet on solidification of
1295 magma ocean. Nature **497**, 607–610 (2013). https://doi.org/10.1038/nature12163
1296 J.K. Harmon, M.A. Slade, Radar mapping of Mercury: full-disk images and polar anomalies.
1297 Science **258,** 640-642 (1992)
1298 Haskin, L.A. and Warren, P.H. Lunar chemistry. In: *Lunar Sourcebook: A User's Guide to the*
1299 *Moon*, (Eds. G. Heiken, D. Vaniman, and B. French) pp. 357–474. New York: Cambridge
1300 University Press. (1991)
1301 S.A. Hauck II, J.L. Margot, S.C. Solomon, R.J. Phillips, C.L. Johnson, F.G. Lemoine, E. Mazarico,
1302 T.J. McCoy, S. Padovan, S.J. Peale, M.E. Perry, D.E. Smith, M.T. Zuber, The curious case of
1303 Mercury's internal structure. J. Geophys. Res.-Planets **118,** 1204-1220 (2013)
1304 E.H. Hauri, A.E. Saal, M. Nakajima, M. Anand, M.J. Rutherford, J.A. Van Orman, M. Le Voyer,
1305 Origin and Evolution of Water in the Moon's Interior. Ann. Rev. Earth Planet. Sci. **45,** 89-111
1306 (2017)
1307 E.H. Hauri, A.E. Saal, M.C. Rutherford, J.A. Van Orman, Water in the Moon's interior: truth and
1308 consequences. Earth Planet. Sci. Lett. **409**, 252–264 (2015)
1309 E.H. Hauri, T. Weinreich, A.E. Saal, M.C. Rutherford, J.A. Van Orman, High pre-eruptive water
1310 contents preserved in lunar melt inclusions. Science **333**, 213–215 (2011)
1311 E. Hauri, J. Wang, J. E. Dixon, P.L. King, C. Mandeville, S. Newman, SIMS analysis of volatiles
1312 in silicate glasses 1. Calibration, matrix effects, and comparisons with FTIR. Chem. Geol.
1313 **183,** 99-114 (2002)
1314 J.W. Head III, L. Wilson, Alphonsus-type dark-halo craters: Morphology, morphometry, and
1315 eruption conditions. Lunar Planet. Sci. Conf. **XI,** 418 (1979).
1316 J.W. Head III, H. Hiesinger, M.A. Ivanov, M.A. Kreslavsky, S. Pratt, B.J. Thomson, Possible
1317 ancient oceans on Mars: evidence from Mars Orbiter Laser Altimeter data. Science **286,** 2134-
1318 2137 (1999)

C.D.K. Herd, Basalts as probes of planetary interior redox state. in *Oxygen in the Solar System* (Ed. G.J. MacPherson), Rev. Mineral. Geochem., **68,** 527-553 (2008)

Y. Higashi, S. Itoh, M. Hashiguchi, S. Sakata, T. Hirata, K. Watanabe, I. Sakaguchi, Hydrogen diffusion in the apatite-water system: fluorapatite parallel to the c-axis. Geochem. J. **51,** 115-122 (2017)

M.M. Hirschmann, A.C. Withers, P. Ardia, N.T. Foley, Solubility of molecular hydrogen in silicate melts and consequences for volatile evolution of terrestrial planets. Earth Planet. Sci. Lett. **345–348**, 38–48 (2012)

L.L. Hood, F. Herbert, C.P. Sonett, The deep lunar electrical conductivity profile: Structural and thermal inferences. J. Geophys. Res. **87,** 5311-5326 (1982)

G.L. Hovis, D.E. Harlov, Solution calorimetric investigation of fluor-chlorapatite crystalline solutions. Amer. Mineral. **95,** 946-952 (2010)

S. Hu, Y. Lin, J. Zhang, J. Hao, L. Feng, L. Xu, W. Yang, J. Yang, NanoSIMS analyses of apatite and melt inclusions in the GRV 020090 Martian meteorite: hydrogen isotope evidence for recent past underground hydrothermal activity on Mars. Geochim. Cosmochim. Acta **140**, 321–333 (2014)

H. Hui, Y. Guan, Y. Chen, A.H. Peslier, Y. Zhang, Y. Liu, R.L. Flemming, G.R. Rossman, J.M. Eiler, C.R. Neal, G.R. Osinsky, A heterogeneous lunar interior for hydrogen isotopes as revealed by the lunar highlands samples. Earth Planet. Sci. Lett. **473**, 14–23, (2017) doi:10.1016/j.epsl.2017.05.029

H. Hui, A.H. Peslier, Y. Zhang, C.R. Neal, Water in lunar anorthosites and evidence for a wet early Moon. Nat. Geosci. (2013) doi:10.1038/ngeo1735

D. Hunten, R.O. Pepin, J.C.G. Walker, Mass fractionation in hydrodynamic escape. Icarus **69,** 532-549 (1987)

A.P. Ingersoll, The runaway greenhouse: a history of water on Venus. J. Atmos. Sci. **26**(6), 1191–1198 (1969)

E. Jarosewich, Chemical analyses of meteorite: A compilation of stony and iron meteorite analyses Meteoritics **25**, 323-337 (1990)

E.A. Jerde, R.V. Morris, P.H. Warren, In quest of lunar regolith breccias of exotic provenance – A uniquely anorthositic sample from the Fra Mauro (Apollo 14) highlands. Earth Planet. Sci. Lett. **98,** 90–108 (1990)

1350 B.L. Jolliff, R.L. Korotev, R.A. Zeigler, C. Floss, Northwest Africa 773: Lunar mare breccia with
1351 a shallow-formed olivine-cumulate component, inferred very-low-Ti (VLT) heritage, and a
1352 KREEP connection. Geochim. Cosmochim. Acta **67,** 4857–4879 (2003)
1353 S.-I. Karato, Some remarks on hydrogen-assisted electrical conductivity in olivine and other
1354 minerals, in: Mibe, K., Kasahara, J. (Eds.), Water in the Earth. Springer, Tokyo. (2017)
1355 S.-I. Karato, Physical basis of trace element partitioning: a review. Am. Mineral. **101**, 2577–2593
1356 (2016)
1357 S.-I. Karato, Geophysical constraints on the water content of the lunar mantle and its implications
1358 for the origin of the Moon. Earth Plan. Sci. Lett. **384**, 144-153 (2013)
1359 S.-I. Karato, D. Wang, Electrical conductivity of minerals and rocks, in *Physics and Chemistry of*
1360 *the Deep Earth*, ed. by S.-I. Karato (Wiley, New York), pp. 145–182 (2013)
1361 J.F. Kasting, J.B. Pollack, Loss of water from Venus, I, Hydrodynamic escape of hydrogen, Icarus
1362 **63**, 479-508 (1983)
1363 C. Kato, F. Moynier, M.C. Valdes, J.K. Dhaliwal, J.M.D. Day, Extensive volatiles loss during the
1364 formation and differentiation of the Moon. Nat. Comm.
1365 http://dx.doi.org/10.1038/ncomms8617 (2015)
1366 A. Kent Jr., Melt inclusions in basaltic and related vol- canic rocks. *Minerals, Inclusions, and*
1367 *Volcanic Processes* (Putirka, K. D. and Tepley, F. J., III, eds.), Rev. Mineral. Geochem. **69**,
1368 273–331, MSA. (2008)
1369 L. Kerber, J.W. Head, D.T. Blewett, S.C. Solomon, L. Wilson, S.L. Murchie, M.S. Robinson, B.
1370 W. Denevi, D.L. Domingue, The global distribution of pyroclastic deposits on Mercury: The
1371 view from MESSENGER flybys 1-3. Planet. Space Sci. **59,** 1895-1909 (2011)
1372 L. Kerber, J.W. Head, S.C. Solomon, S.L. Murchie, D.T. Blewett, L. Wilson, Explosive volcanic
1373 eruptions on Mercury: Eruption conditions, magma volatile content, and implications for
1374 interior volatile abundances. Earth Planet. Sci. Lett. **285,** 263-271 (2009)
1375 K. Kitts, K. Lodders, Survey and evaluation of eucrite bulk compositions. Meteor. Plan. Sci. **33**,
1376 A197–A213 (1998)
1377 T. Kleine, M. Touboul, B. Bourdon, F. Nimmo, K. Mezger, H. Palme, S.B. Jacobsen, Q-Z. Yin,
1378 A.N. Halliday, Hf-W chronology of the accretion and evolution of asteroids and terrestrial
1379 planets. Geochim. Cosmochim. Acta **73,** 5150-5188 (2009)

1380 R.L. Korotev, Mixing levels, the Apennine Front soil component, and compositional trends in the
1381 Apollo 15 soils. Proc. Lunar Plan. Sci. Conf. **17**, E411–E431 (1987)
1382 R.L. Korotev, D.T. Kremser, Compositional variations in Apollo 17 soils and their relationship to
1383 the geology of the Taurus-Littrow site. Proc. Lunar Plan. Sci. Conf. **22**, 275–301 (1992)
1384 H. Kurokawa, M. Sato, M. Ushioda, T. Matsuyama, R. Moriwaki, J.M. Dohm, T. Usui, Evolution
1385 of water reservoirs on Mars: Constraints from hydrogen isotopes in martian meteorites. Earth
1386 Plan. Sci. Lett. **394**, 179-185 (2014)
1387 V. Lainey, V. Dehant, M. Pätzold, First numerical ephemerides of the Martian moons. Astron.
1388 Astrophys. **465,** 1075-1084 (2007)
1389 D.J. Lawrence, W.C. Feldman, J.O. Goldsten, S. Maurice, P.N. Peplowski, B.J. Anderson, D.
1390 Bazell, R.L. McNutt Jr., L.R. Nittler, T.H. Prettyman, D.J. Rodgers, S.C. Solomon, S.Z.
1391 Weider, Evidence for water ice near Mercury's north pole from MESSENGER neutron
1392 spectrometer measurements. Science **339,** 292-298 (2013)
1393 L.A. Leshin, Insights into martian water reservoirs from analyses of martian meteorite QUE94201.
1394 Geophys. Res. Lett. **27,** 2017-2020 (2000)
1395 L. A. Leshin, P. R. Mahaffy, C. R. Webster, M. Cabane, P. Coll, P. G. Conrad, P. D. Archer Jr., S.
1396 K. Atreya, A. E. Brunner, A. Buch, J. L. Eigenbrode, G. J. Flesch, H. B. Franz, C.
1397 Freissinet, D. P. Glavin, A. C. Mcadam, K. E. Miller, D. W. Ming, R. V. Morris, R. Navarro-
1398 González, P. B. Niles, T. Owen, R. O. Pepin, S. Squyres, A. Steele, J. C. Stern, R. E.
1399 Summons, D. Y. Sumner, B. Sutter, C. Szopa, S. Teinturier, M. G. Trainer, J. J. Wray, J. P.
1400 Grotzinger, MSL Science Team, Volatile, isotope, and organic analysis of Martian fines with
1401 the Mars Curiosity rover. Science **341,** 1238937 (2013)
1402 Y. Liu, C. Ma, J.R. Beckett, Y. Chen, Y. Guan, Rare-earth element minerals in martian meteorites
1403 NWA 7034 and 7533: Implications for fluid-rock interaction in the martian crust. Earth Planet.
1404 Sci. Lett. **451,** 251-262 (2016)
1405 Y. Liu, Y. Guan, Y. Zhang, G.R. Rossman, J.M. Eiler, L.A. Taylor, Direct measurement of
1406 hydroxyl in the lunar regolith and the origin of lunar surface water. Nature Geosci. **5,** 779-782
1407 (2012)
1408 S.J. Lock, S.T. Stewart, M.I. Petaev, Z.M. Leinhardt, M.T. Mace, S.B. Jacobsen, M. Ćuk, The
1409 origin of the Moon within a terrestrial synestia. J. Geophys. Res. (2018)
1410 https://doi.org/10.1002/2017JE005333

K. Lodders, B. Fegley, *The Planetary Scientist's Companion*, Oxford University Press, New York (1998)

P. Lowell, *Mars and its Canals*, Macmillan, London (1906)

P. Lucey, R.L. Korotev, J.J. Gillis, L.A. Taylor, D. Lawrence, B.A. Campbell, R. Elphic, B. Feldman, L.L. Hood, D. Hunten, M. Mendillo, S. Noble, J.J. Papike, R.C. Reedy, S. Lawson, T. Prettyman, O. Gasnault, S. Maurice, Understanding the lunar surface and Space–Moon interactions, in *New Views of the Moon*, (Eds. B.L. Joliff, M.A. Weiczorek, C.K. Shearer, C.R. Neal), Rev. Min. Geochem. **60**, 83–219 (2006)

R.W. Luth, Mantle volatiles-distributions and consequences, in *The Mantle and Core* (ed. R. W. Carlson), *Treatise on Geochemistry*, Elsevier-Pergamon, Oxford, pp. 319-361 (2005)

P. R. Mahaffy, C. R. Webster, J. C. Stern, A. E. Brunner, S. K. Atreya, P. G. Conrad, S. Domagal-Goldman, J. L. Eigenbrode, G. J. Flesch, L. E. Christensen, H. B. Franz, C. Freissinet, D. P. Glavin, J. P. Grotzinger, J. H. Jones, L. A. Leshin, C. Malespin, A. C. Mcadam, D. W. Ming, R. Navarro-Gonzalez, P. B. Niles, T. Owen, A. A. Pavlov, A. Steele, M. G. Trainer, K. H. Williford, J. J. Wray, The MSL Science Team, The imprint of atmospheric evolution in the D/H of Hesperian clay minerals on Mars. Science **347**, 412-414 (2015)

V. Malavergne, M.J. Toplis, S. Berthet, J. Jones, Highly reducing conditions during core formation on Mercury: Implications for internal structure and the origin of a magnetic field. Icarus **206,** 199-209 (2010)

V. Malavergne, J. Siebert, F. Guyot, L. Gautron, R. Combes, T. Hammouda, S. Borensztajn,D. Frost, I. Martinez, Si in the core? New high-pressure and high-temperature experimental data. Geochim. Cosmochim. Acta **68,** 4201-4211 (2004)

B.E. Mandler, L.T. Elkins-Tanton, The origin of eucrites, diogenites, and olivine diogenites: magma ocean crystallization and shallow magma chamber processes on Vesta. Meteorit. Planet. Sci. **48**, 2333–2349, (2013)

P. Mane, R. Hervig, M. Wadhwa, L.A.J. Garvie, J.B. Balta, H.Y. McSween Jr., Hydrogen isotopic composition of the Martian mantle inferred from the newest Martian meteorite fall, Tissint. Meteor. Planet. Sci. **1-9,** (2016) doi: 10.1111/maps.12717

B. Marty, G. Avice, Y. Sano, K. Altwegg, H. Balsiger, M. Hässig, A. Morbidelli, O. Mousis, M. Rubie, Origins of volatile elements (H, C, N, noble gases) on Earth and Mars in light of recent results from the ROSETTA cometary mission. Earth Planet. Sci. Lett. **441**, 91–102 (2016)

1442 B. Marty, The origins and concentrations of water, carbon, nitrogen and noble gases on Earth.
1443 Earth Planet. Sci. Lett. **313-314,** 56-66 (2012)
1444 T.J. McCoy, T.L. Dickinson, G.E. Lofgren, Partial melting of the Indarch (EH4) meteorite: A
1445 textural, chemical, and phase relations view of melting and melt migration. Meteor. Planet.
1446 Sci. **34,** 735-746 (1999)
1447 F.M. McCubbin, K.E. Vander Kaaden, P.N. Peplowski, A.S. Bell, L.R. Nittler, J.W. Boyce, L.G.
1448 Evans, L.P. Keller, S.M. Elardo, T.J. McCoy, A low O/Si ratio on the surface of Mercury:
1449 Evidence for silicon smelting? J. Geophys. Res. **122,** 2053-2076 (2017)
1450 F.M. McCubbin, K.E. Vander Kaaden, R. Tartése, R.L. Klima, Y. Liu, J. Mortimer, J.J. Barnes,
1451 C.K. Shearer, A.H. Treiman, D.J. Lawrence, S.M. Elardo, D.M. Hurley, J.W. Boyce, and M.
1452 Anand, Magmatic volatiles (H, C, N, F, S, Cl) in the lunar mantle, crust, and regolith:
1453 Abundances, distributions, processes, and reservoirs. Am. Mineral. **100,** 1668-1707 (2015a)
1454 F.M. McCubbin, K.E. Vander Kaaden, R. Tartèse, J.W. Boyce, S. Mikhail, E.S. Whitson, A.S.
1455 Bell, M. Anand, I.A. Franchi, J. Wang, E.H. Hauri, Experimental investigation of F, Cl, and
1456 OH partitioning between apatite and Fe-rich basaltic melt at 1.0–1.2 GPa and 950–1000°C.
1457 Amer. Mineral. **100,** 1790–1802 (2015b)
1458 F.M. McCubbin, M.A. Riner, K.E. Vander Kaaden, L.K. Burkemper, Is Mercury a volatile-rich
1459 planet? Geophys. Res. Lett. **39,** (2012a)
1460 F.M. McCubbin, E.H. Hauri, S.M. Elardo, K.E. Vander Kaaden, J. Wang, C.K. Shearer Jr.,
1461 Hydrous melting of the martian mantle produced both depleted and enriched shergottites.
1462 Geology doi:10.1130/G33242.1. (2012b)
1463 F.M. McCubbin, A. Steele, E.H. Hauri, H. Nekvasil, S. Yamashita, R.J. Hemley, Nominally
1464 hydrous magmatism on the Moon. Proc. Nat. Acad. Sci. **107.25,** 11223-11228 (2010a)
1465 F.M. McCubbin, A. Steele, H. Nekvasil, A. Schnieders, T. Rose, M. Fries, P.K. Carpenter, B.L.
1466 Jolliff, Detection of structurally bound hydroxyl in fluorapatite from Apollo Mare basalt
1467 15058,128 using TOF-SIMS. Amer. Mineral. **95,** 1141-1150 (2010b)
1468 W.F. McDonough, S.-S. Sun, The composition of the Earth. Chem. Geol. **120**, 223–253 (1995)
1469 M.B. McElroy, Y.L. Yung, A.O. Nier, Isotopic composition of nitrogen: Implications for the past
1470 history of Mars' atmosphere. Science **194,** 70-72 (1976)

W.B. McKinnon, K.J. Zahnle, B.A. Ivanov, H.J. Melosh, Cratering on Venus: Models and observations, in *Venus II,* (Eds. S.W. Bougher, D.M. Hunten, R.J. Phillips) pp. 969-1014, Univ. of Ariz. Press, Tucson. (1997)

H. Y. McSween Jr., R.P. Binzel, M.C. De Sanctis, E. Ammannito, T.H. Prettyman, A.W. Beck, V. Reddy, L. Le Corre, M.J. Gaffey, T.B. McCord, C.A. Raymond, C.T. Russell, the Dawn Science Team, Dawn; the Vesta–HED connection; and the geologic context for eucrites, diogenites, and howardites. Meteorit. Plan. Sci. **48,** 2090-2104 (2013)

L. Merlivat, M. Lelu, G. Nief, E. Roth, Spallation deuterium in rock 70215. Proc. Lunar Sci. Conf. **7,** 649-658 (1976)

F. Montmessin, T. Fouchet, F. Forget, Modeling the annual cycle of HDO in the Martian atmosphere. J. Geophys. Res. **110**, E03006 (2005)

A. Morbidelli, J.I. Lunine, D.P. O'Brien, S.N. Raymond, K.J. Walsh, Building terrestrial planets. Ann. Rev. Earth Planet. Sci. **40**, 251–275, (2012) https://doi.org/10.1146/annurevearth042711-105319

J. Mortimer, A.B. Verchovsky, M. Anand, I. Gilmour, C.T. Pillinger, Simultaneous analysis of abundance and isotopic composition of nitrogen, carbon, and noble gases in lunar basalts: insights into interior and surface processes on the Moon. Icarus (2015) http://dx.doi.org/10.1016/j.icarus.2014.10.006

J. Mouginot, A. Pommerol, P. Beck, W. Kofman, S.M. Clifford, Dielectric map of the Martian northern hemisphere and the nature of plain filling materials. Geophys. Res. Lett. **39,** L02202 (2012)

S.L. Murchie, R.L. Klima, B.W. Denevi, C.M. Ernst, M.R. Keller, D.L. Domingue, D.T. Blewett, N.L. Chabot, C. Hash, E. Malaret, N.R. Izenberg, F. Vilas, L.R. Nittler, J.W. Head, Orbital multispectral mapping of Mercury using the MESSENGER Mercury Dual Imaging System: Evidence for the origins of plains units and low-reflectance material. Icarus **254,** 287-305 (2015)

N. Muttik, F.M. McCubbin, L.P. Keller, A.R. Santos, W.A. McCutcheon, P.P. Provencio, Z. Rahman, C.K. Shearer, J.W. Boyce, C.B. Agee, Inventory of H_2O in the ancient martian regolith from Northwest Africa 7034: The important role of iron oxides. Geophys. Res. Lett. **41,** 8235–8244, doi:10.1002/2014GL062533 (2014)

M. Nakajima, D.J. Stevenson, Inefficient volatile loss from the Moon-forming disk: Reconciling the giant impact hypothesis and a wet Moon. Earth and Planetary Science Letters **487,** 117-126 (2018)

O. Namur, M. Collinet, B. Charlier, T.L. Grove, F. Holtz, C. McCammon, Melting processes and mantle sources of surface lavas on Mercury. Earth Planet. Sci. Lett. **439,** (2016)

H.E. Newson, W.M. White, K.P. Jochum, A.W. Hofmann, Siderophile and chalcophile element abundances in oceanic basalts, Pb isotope evolution and growth of the Earth's core. Earth Planet. Sci. Lett. **80**, 299–313 (1986)

A.O. Nier, M.B. McElroy, Y.L. Yung, Isotopic composition of the Martian atmosphere. Science **194,** 68-70 (1976)

L.R. Nittler, R.D. Starr, S.Z. Weider, T.J. McCoy, W.V. Boynton, D.S. Ebel, C.M. Ernst, L.G. Evans, J.O. Goldsten, D.K. Hamara, D.J. Lawrence, R.L. McNutt, C.E. Schlemm, S.C. Solomon, A.L. Sprague, The Major-Element Composition of Mercury's Surface from MESSENGER X-ray Spectrometry. Science **333,** 1847-1850 (2011)

L.E., Nyquist, C-Y. Shih, F.M. McCubbin, A.R. Santos, C.K. Shearer, Z.X. Peng, P.V. Burger, C.B. Agee, Rb-Sr and Sm-Nd isotopic and REE studies of igneous components in the bulk matrix domain of Martian breccia Northwest Africa 7034. Meteorit. Plan. Sci. **51**, 483-498 (2016)

D.P. O'Brien, A. Izidoro, S.A. Jacobson, S.N. Raymond, D.C. Rubie, The delivery of water during terrestrial planet formation. Space Sci. Rev. **214,** 47 (this book) (2018) https://doi.org/10.1007/s11214-018-0475-8

J. Ormö, J.M. Dohm, J.C. Ferris, A. Lepinette, A.G. Fairén, Marine ‐ target craters on Mars? An assessment study. Meteor. Planet. Sci**. 39,** 333-346 (2004)

T. Owen, The composition and early history of the atmosphere of Mars. In *Mars* (eds. H. H. Kieffer, Jakosky, B. M. and Snyder, C. W.) U. Arizona Press, Tucson, AZ (1992)

T. Owen, J.P. Maillard, C. de Bergh, B.L. Lutz, Deuterium on Mars: The abundance of HDO and the value of D/H. Science **240**, 1767-1770 (1988)

K. Pahlevan, D.J. Stevenson, Volatile loss Following the Moonforming giant impact. Geochim. Cosmochim. Acta Suppl. **72,** A716. (2008)

K. Pahlevan, S.-I. Karato, B. Fegley, Speciation and dissolution of hydrogen in the proto-lunar disk. Earth Planet. Sci. Lett. **445,** 104-113 (2016)

H. Palme, H.S.C. O'Neill, Cosmochemical estimates of mantle composition, in *The Mantle and Core* (ed. R. W. Carlson), *Treatise on Geochemistry*, Elsevier-Pergamon, Oxford, pp. 1–39 (2014)

Y.M. Pan, M.E. Fleet, Compositions of the apatite-group minerals: Substitution mechanisms and controlling factors, in *Phosphates: Geochemical, Geobiological, and Materials Importance.* (Eds: M.J. Kohn, J. Rakovan, J.M. Hughes) Rev. Min. Geochem. **48,** pp. 13-49 (2002)

R.C. Paniello, J.M.D. Day, F. Moynier, Zinc isotope evidence for the origin of the Moon. Nature **490,** 376-380 (2012)

S.W. Parman, E.M. Parmentier, S. Wang, Crystallization of Mercury's sulfur-rich magma ocean. Lunar Planet. Sci. Conf. **XLVII,** abstract# 2990, (2016)

E.M. Parmentier, P.C. and Hess, Chemical differentiation of a convecting planetary interior: Consequences for a one plate planet such as Venus. Geophys. Res. Lett. **19,** 2015–2018 (1992)

P.N. Peplowski, R.L. Klima, D.J. Lawrence, C.M. Ernst, B.W. Denevi, E.A. Frank, J.O. Goldsten, S.L. Murchie, L.R. Nittler, S.C. Solomon, S.C., Remote sensing evidence for an ancient carbon-bearing crust on Mercury. Nature Geosci. **9,** 273-276 (2016)

P.N. Peplowski, D.J. Lawrence, L.G. Evans, R.L. Klima, D.T. Blewett, J.O. Goldsten, S.L. Murchie, T.J. McCoy, L.R. Nittler, S.C. Solomon, R.D. Starr, S.Z. Weider, Constraints on the abundance of carbon in near-surface materials on Mercury: Results from the MESSENGER Gamma-Ray Spectrometer. Plan. Space Sci. **108,** 98-107 (2015)

P.N. Peplowski, L.G. Evans, K.R. Stockstill-Cahill, D.J. Lawrence, J.O. Goldsten, T.J. McCoy, L.R. Nittler, S.C. Solomon, A.L. Sprague, R.D. Starr, S.Z. Weider, Enhanced sodium abundance in Mercury's north polar region revealed by the MESSENGER Gamma-Ray Spectrometer. Icarus **228,** 86-95 (2014)

P.N. Peplowski, D.J. Lawrence, E.A. Rhodes, A.L. Sprague, T.J. McCoy, B.W. Denevi, L.G. Evans, J.W. Head, L.R. Nittler, S.C. Solomon, K.R. Stockstill-Cahill, S.Z. Weider, Variations in the abundances of potassium and thorium on the surface of Mercury: Results from the MESSENGER Gamma-Ray Spectrometer. J. Geophys. Res. **117,** E00L04, (2012) doi:10.1029/2012JE004141

P.N. Peplowski, L.G. Evans, S.A. Hauck, T.J. McCoy, W.V. Boynton, J.J. Gillis-Davis, D.S. Ebel, J.O. Goldsten, D.K. Hamara, D.J. Lawrence, R.L. McNutt, L.R. Nittler, S.C. Solomon, E.A. Rhodes, A.L. Sprague, R.D. Starr, K.R. Stockstill-Cahill, K.R., Radioactive elements on

1563 Mercury's surface from MESSENGER: Implications for the planet's formation and evolution.
1564 Science **333,** 1850-1852 (2011)
1565 A.H. Peslier, M. Schönbächler, H. Busemann, S.I. Karato, Water in the Earth's interior:
1566 distribution and origin. Space Sci. Rev. **212**, (this book) 743–810,
1567 https://doi.org/10.1007/s11214-017-0387-z (2017)
1568 A.E. Potter, T.H. Morgan, Potassium in the atmosphere of Mercury. Icarus **67**, 336–340 (1986)
1569 A.E. Potter, T.H. Morgan, Discovery of sodium in the atmosphere of Mercury. Science **229**, 651–
1570 653 (1985)
1571 B. Rava, B. Hapke, An analysis of the Mariner 10 color ratio map of Mercury. Icarus **71,** 397-429
1572 (1987)
1573 R.C. Reedy, Cosmic-ray produced stable nuclides: Various production rates and their implications.
1574 Lunar Planet. Sci Conf. **XII,** 871 (1981)
1575 J. Riker, M.C.S. Humphreys, R.A. Brooker, J.C.M. De Hoog, EIMF, First measurements of OH-
1576 C exchange and temperature-dependent partitioning of OH and halogens in the system apatite
1577 – silicate melt. Amer. Mineral. **103,** 260-270 (2018)
1578 M.A. Riner, P.G. Lucey, S.J. Desch, F.M. McCubbin, Nature of opaque components on Mercury:
1579 Insights into a Mercurian magma ocean. Geophys. Res. Lett. **36,** (2009)
1580 K.L. Robinson, G.J. Taylor, Heterogeneous distribution of water in the Moon. Nat. Geosci. **7,**
1581 401-408 (2014)
1582 K.L. Robinson, J.J. Barnes, K. Nagashima, A. Thomen, I.A. Franchi, G.R. Huss, M. Anand, G.J.
1583 Taylor, Water in evolved lunar rocks: Evidence for multiple reservoirs. Geochim. Cosmochim.
1584 Acta **188,** 244-260 (2016)
1585 M.S. Robinson, S.L. Murchie, D.T. Blewett, D.L. Domingue, S.E. Hawkins, J.W. Head III, G.M.
1586 Holsclaw, W.E. McClintock, T.J. McCoy, R.L. McNutt Jr., L.M. Prockter, S.C. Solomon, T.R.
1587 Watters, Reflectance and color variations on Mercury: Regolith processes and compositional
1588 heterogeneity. Science **321,** 66-69 (2008)
1589 D.C. Rubie, D.J. Frost, U. Mann, Y. Asahara, F. Nimmo, K. Tsuno, P. Kegler, A. Holzheid, H.
1590 Palme, Heterogeneous accretion, composition and core-mantle differentiation of the Earth.
1591 Earth Planet. Sci. Lett. **301**, 31–42, (2011) https://doi.org/10.1016/j.epsl.2010.11.030

A.E. Saal, E.H. Hauri, M. Lo Cascio, J.A. Van Orman, M.C. Rutherford, R.F. Cooper, Volatile content of lunar volcanic glasses and the presence of water in the Moon's interior. Nature **454**, 192–196 (2008)

A.E. Saal, E.H. Hauri, J.A. Van Orman, M.C. Rutherford, Hydrogen isotopes in lunar volcanic glasses and melt inclusions reveal a carbonaceous chondrite heritage. Science **340**, 1317–1320 (2013)

J. Salmon, R.M. Canup, Lunar accretion from a Roche-interior fluid disk. Astrophys. J. **760,** 10.1088/0004-1637X/1760/1081/1083. (2012)

C. Sanloup, A. Jambon, P. Gillet, A simple chondritic model of Mars. Phys. Earth Plan. Int. **112,** 43-54 (1999)

A.R. Sarafian, S.G. Nielsen, H.R. Marschall, F.M. McCubbin, B.D. Monteleone, Early accretion of water in the inner solar system from a carbonaceous chondrite-like source. Science **346**, 623–626 (2014)

A.R. Sarafian, E.H. Hauri, F.M. McCubbin, T.J. Lapen, E.L. Berger, S.G. Nielsen, H.R. Marschall, G.A. Gaetani, K. Righter, E. Sarafian, Early accretion of water and volatile elements to the inner Solar System: evidence from angrites. Philos. Trans. R. Soc. Lond. A **375**, 1–27 (2017)

G.G. Schaber, R.G., Strom, H.J. Moore, L.A. Soderblom, R.L. Kirk, D.J. Chadwick, D.D. Dawson, L. R. Gaddis, J.M. Boyce, J. Russell, Geology and distribution of impact craters on Venus: What are they telling us? J. Geophys. Res. **97,** 13257–13301(1992)

Z.D. Sharp, Principles of stable isotope geochemistry. 2nd ed. doi:10.5072/FK2GB24S9F (2017)

Z.D. Sharp, F.M. McCubbin, C.K. Shearer, A hydrogen-based oxidation mechanism relevant to planetary formation. Earth Planet. Sci. Lett. **380**, 88–97 (2013)

Z.D. Sharp, C.K. Shearer, K.D. McKeegan, J.D. Barnes, Y.Q. Wang, The chlorine isotope composition of the Moon and implications for an anhydrous mantle. Science **329,** 1050-1053 (2010)

J.A. Singer, J.P. Greenwood, S. Itoh, N. Sakamoto, H. Yurimoto, Evidence for the solar wind in lunar magmas: A study of slowly-cooled samples of the Apollo 12 olivine basalt suite. Geochem J. **51,** 95-104 (2017)

M.A. Slade, B.J. Butler, D.O. Muhleman, Mercury radar imaging: evidence for polar ice. Science **258,** 635-640 (1992)

1622 G. Slodzian, T.D. Wu, N. Bardin, J. Duprat, C. Engrand, J.L. Guerquin-Kern, Simultaneous
1623 hydrogen and heavier element isotopic ratio images with a scanning submicron ion probe and
1624 mass resolved polyatomic ions. Microsc. Microanal. **20(2),** 577-581 (2014)
1625 D.E. Smith, M.T. Zuber, R.J. Phillips, S.C. Solomon, S.A. Hauck, F.G., Lemoine, E. Mazarico,
1626 G.A. Neumann, S.J. Peale, J.–L. Margot, C.L. Johnson, M.H., Torrence, M.E. Perry, D.D.
1627 Rowlands, S. Goossens, J.W. Head, A.H. Taylor, Gravity field and internal structure of
1628 Mercury from MESSENGER. Science **336,** 214-217 (2012)
1629 P. H. Smith, L. K. Tamppari, R. E. Arvidson, D. Bass, D. Blaney, W. V. Boynton, A. Carswell, D.
1630 C. Catling, B. C. Clark, T. Duck, E. DeJong, D. Fisher, W. Goetz, H. P. Gunnlaugsson, M. H.
1631 Hecht, V. Hipkin, J. Hoffman, S. F. Hviid, H. U. Keller, S. P. Kounaves, C. F. Lange, M. T.
1632 Lemmon, M. B. Madsen, W. J. Markiewicz, J. Marshall, C. P. McKay, M. T. Mellon, D. W.
1633 Ming, R. V. Morris, W. T. Pike, N. Renno, U. Staufer, C. Stoker, P. Taylor, J. A. Whiteway,
1634 A. P. Zent, H_2O at the Phoenix Landing Site. Science **325,** 58-61. (2009)
1635 DOI:10.1126/science.1172339
1636 S.C. Solomon, R.L. McNutt Jr., R.E. Gold, M.H. Acuña, D.N. Baker, W.V. Boynton, C.R.
1637 Chapman, A.F. Cheng, G. Gloeckler, J.W. Head, S.M. Krimigis, W.E. McClintock, S.L.
1638 Murchie, S.J. Peale, R.J. Phillips, M.S. Robinson, J.A. Slavin, D.E. Smith, R.G. Strom, J.I.
1639 Trombka, M.T. Zuber, The MESSENGER mission to Mercury: Scientific objectives and
1640 implementation. Plan. Space Sci. **49,** 1445-1465 (2001)
1641 C.P. Sonett, D.S. Colburn, P. Dyal, C.W. Parkin, B.F. Smith, G. Schubert, K. Schwartz, Lunar
1642 electrical conductivity profile. Nature **230**, 359-362 (1971)
1643 D.J. Stevenson, Origin of the Moon - the Collision Hypothesis. Ann. Rev. Earth Plan. Sci. **15,** 271-
1644 315 (1987)
1645 K.R. Stockstill-Cahill, T.J. McCoy, L.R. Nittler, S.Z. Weider, S.A. Hauck II, Magnesium-rich
1646 crustal compositions on Mercury: Implications for magmatism from petrologic modeling. J.
1647 Geophys. Res. **117,** E00L15 (2012)
1648 N. Sugiura, H. Hoshino, Hydrogen-isotopic compositions in Allan Hills 84001 and the evolution
1649 of the martian atmosphere. Meteor. Planet. Sci. **35,** 373-380 (2000)
1650 R. Tartése, M. Anand, Late delivery of chondritic hydrogen into the lunar mantle: Insights from
1651 mare basalts. Earth Planet. Sci. Lett. **361,** 480-486 (2013)

1652 R. Tartèse M. Anand, F.M. McCubbin, S.M. Elardo, C.K. Shearer, and I.A. Franchi, Apatite in
1653 lunar KREEP basalts: The missing link to understanding the H isotope systematics of the
1654 Moon. Geology **42**, 363-366 (2014a)
1655 R. Tartèse, M. Anand, K.H. Joy, I.A. Franchi, H and Cl isotope systematics of apatite in brecciated
1656 lunar meteorites Northwest Africa 4472, 773, Sayh al Uhaymir 169, and Kalahari 009. Meteor.
1657 Planet. Sci. **1-24**, doi: 10.1111/maps.12398 (2014b)
1658 R. Tartèse, M. Anand, J.J. Barnes, N.A. Starkey, I.A. Franchi, Y. Sano, The abundance,
1659 distribution, and isotopic composition of hydrogen in the Moon as revealed by basaltic lunar
1660 samples: Implications for the volatile inventory of the Moon. Geochim. Cosmochim. Acta
1661 **122,** 58-74 (2013)
1662 B.E. Taylor, Magmatic volatiles: Isotopic variation of C, H, and S. In *Stable Isotopes in high*
1663 *temperature geological processes.* (Eds. J. W. Valley, H. P. Taylor, Jr., J. R. O'Neil) Rev. Min.
1664 16, MSA, Blacksburg, VA (1986)
1665 G.J. Taylor, The bulk composition of Mars. Chemie der Erde **73**, 401–420 (2013)
1666 R.J. Thomas, D.A. Rothery, S.J. Conway, M. Anand, Explosive volcanism in complex impact
1667 craters on Mercury and the Moon: Influence of tectonic regime on depth of magmatic intrusion.
1668 Earth Plan. Sci. Lett. **431,** 164-172 (2015)
1669 R.J. Thomas, D.A. Rothery, S.J. Conway, M. Anand, Long-lived explosive volcanism on Mercury.
1670 Geophys. Res. Lett. **41,** 6084-6092 (2014)
1671 A. Treiman, E. Harrington, V. Sharpton, Venus' radar bright highlands: Different signatures and
1672 materials on Ovda Regio and on Maxwell Montes, Icarus **280**, 172-182 (2016a)
1673 A.H. Treiman, J.W. Boyce, J.P. Greenwood, J.M. Eiler, J. Gross, Y. Guan, C. Ma, and E.M.
1674 Stolper, D-poor hydrogen in lunar mare basalts assimilated from lunar regolith. Amer. Mineral.
1675 101, 1596-1603. (2016b)
1676 J. Tuff, J. Wade, B. Wood, Volcanism on Mars controlled by early oxidation of the upper mantle.
1677 Nature **498,** 342 (2013)
1678 G. Ustunisik, H. Nekvasil, D.H. Lindsley, F.M. McCubbin, Degassing pathways of Cl-, F-, H-,
1679 and S-bearing magmas near the lunar surface: Implications for the composition and Cl isotopic
1680 values of lunar apatite. Am. Mineral. **100(8-9),** 1717-1727 (2015)
1681 T. Usui, Hydrogen reservoirs in Mars as revealed by martian meteorites. In *Volatiles in the*
1682 *Martian crust*. (Eds. J. Filiberto, S. S. Schwenzer). Elsevier, Amsterdam (2018)

1683 T. Usui, C.M.O.D. Alexander, J. Wang, J.I. Simon, J.H. Jones, Origin of water and mantle-crust
1684 interactions on Mars inferred from hydrogen isotopes and volatile element abundances of
1685 olivine-hosted melt inclusions of primitive shergottites. Earth Planet. Sci. Lett. **357–358**, 119–
1686 129 (2012)
1687 T. Usui, C.M.O.D. Alexander, J. Wang, J.I. Simon, J.H. Jones, Meteoritic evidence for a
1688 previously unrecognized hydrogen reservoir on Mars. Earth Planet. Sci. Lett. **410**, 140–151
1689 (2015)
1690 K.E. Vander Kaaden, F.M. McCubbin, The origin of boninites on Mercury: An experimental study
1691 of the northern volcanic plains lavas. Geochim. Cosmochim. Acta **173,** 246-263 (2016)
1692 K.E. Vander Kaaden, F.M. McCubbin, Exotic crust formation on Mercury: Consequences of a
1693 shallow, FeO-poor mantle. J. Geophys. Res. **120,** 195-209 (2015)
1694 K.E. Vander Kaaden, F.M. McCubbin, L.R. Nittler, P.N. Peplowski, S.Z. Weider, E.A. Frank, T.J.
1695 McCoy, Geochemistry, mineralogy, and petrology of boninitic and komatiitic rocks on the
1696 mercurian surface: Insights into the mercurian mantle. Icarus **285,** 155-168 (2017)
1697 K.E. Vander Kaaden, F.M. McCubbin, D.K. Ross, J.F. Rapp, L.R. Danielson, L.P. Keller, K.
1698 Righter, 2016. Carbon solubility in Si-Fe-bearing metals during core formation on Mercury,
1699 Lunar Plan. Sci. Conf. **XLVII,** abstract# 1474, (2016)
1700 O. Verhoeven, P. Vasher, Laboratory-based electrical conductivity at Martian mantle conditions.
1701 Plan. Space Sci. **134**, 29-35 (2016)
1702 G.L. Villanueva, M.J. Mumma, R.E. Novak, H.U. Käufl, P. Hartogh, T. Encrenaz, A. Tokunaga,
1703 A. Khayat, M.D. Smith, Strong water isotopic anomalies in the martian atmosphere: Probing
1704 current and ancient reservoirs. Science **348**, 218-221 (2015)
1705 M. Wadhwa, Redox conditions on small bodies, the Moon, and Mars. in *Oxygen in the Solar*
1706 *System* (Ed. G.J. MacPherson), Rev. Mineral. Geochem., **68,** 493-510 (2008)
1707 D. Walker, J. Longhi, J. Kirkpatrick, J.F. Hays, Differentiation of an Apollo 12 picrite magma.
1708 Proc. Lunar Planet. Sci. Conf. **7**, 1365–1389 (1976)
1709 K.J. Walsh, A. Morbidelli, S.N. Raymond, D.P. O'Brien, A.M. Mandell, A low mass for Mars
1710 from Jupiter's early gas-driven migration. Nature **475**, 206–209, (2011)
1711 https://doi.org/10.1038/nature10201
1712 K. Wang, S.B. Jacobsen, Potassium isotopic evidence for a high-energy giant impact origin of the
1713 Moon. Nature **538,** 487 (2016)

H. Wänke, G. Dreibus. Chemical composition and accretion history of terrestrial planets. Philos. Trans. R. Soc. London, Ser. A, **325,** 545-557 (1988)

P.H. Warren, "New" lunar meteorites: Implications for composition of the global lunar surface, of the lunar crust, and of the bulk Moon. Meteorit. Plan. Sci. **40**, 477–506 (2005)

P.H. Warren, The magma ocean concept and lunar evolution. Ann. Rev. Earth Plan. Sci. **13,** 201-240 (1985)

P.H. Warren, G.J. Taylor, The Moon. In: *Planets, Asteroids, Comets, and the Solar System*, (Ed. A.M. Davis) In: *Treatise on Geochemistry*, 2nd ed., pp. 213–250, (2014)

P.H. Warren, G.W. Kallemeyn, Geochemistry of lunar meteorite Yamato-791197: Comparison with ALHA81005 and other lunar samples. *Proceedings of the NIPR Symposium on Antarctic Meteorites (Tokyo)*, **vol. 10**, pp. 3–16 (1986)

P.H. Warren, J.T. Wasson, The origin of KREEP. Rev. Geophys. Space Phys. **17**, 73-88.

J.T. Wasson, G.W. Kallemeyn, Compositions of chondrites. Philos. Trans. R. Soc. Lond. **A325**, 535–544 (1988)

L.L. Watson, I.D. Hutcheon, S. Epstein, E.M. Stolper, Water on Mars: clues from deuterium/hydrogen and water contents of hydrous phases in SNC meteorites. Science **265**, 86–90 (1994)

C.R. Webster, P.R. Mahaffy, G.J. Flesch, P.B. Niles, J.H. Jones, L.A. Leshin, S.K. Atreya, J.C. Stern, L.E. Christensen, T. Owen, H. Franz, R.O. Pepin, A. Steele, The MSL Science Team, Isotope ratios of H, C, and O in CO_2 and H_2O of the martian atmosphere. Science **341**, 260-263 (2013)

S.Z. Weider, L.R. Nittler, R.D. Starr, T.J. McCoy, K.R. Stockstill-Cahill, P.K. Byrne, B.W. Denevi, J.W. Head, S.C. Solomon, Chemical heterogeneity on Mercury's surface revealed by the MESSENGER X-Ray Spectrometer. J. Geophys. Res. **117,** (2012) https://doi.org/10.1029/2012JE004153

J.G. Williams, D.H. Boggs, C.F. Yoder, J.T. Ratcliff, J.O. Dickey, Lunar rotational dissipation in solid body and molten core. J. Geophys. Res. **106,** 27933–27968 (2001)

B.J. Wood, A.N. Halliday, M. Rehkamper, Volatile accretion history of the Earth. Nature **467**, E6–E7 (2010)

R.D. Wordsworth, The climate of early Mars. Ann. Rev. Earth Planet. Sci. **44,** 381-408 (2016)

Y. Xu, T.J. Shankland, A.G. Duba, Pressure effect on electrical conductivity of mantle olivine. Phys. Earth Planet. Int. **118,** 149-161 (2000)

T. Yoshino, A. Shimojuku, S. Shan, X. Guo, D. Yamazaki, E. Ito, Y. Higo, K. Funakoshi, Effect of temperature, pressure and iron content on the electrical conductivity of olivine and its high-pressure polymorphs. J. Geophys. Res. **117,** (2012) doi:2011JB008774

E.D. Young, Evaporating planetesimals. Nature **549,** 461-462 (2017)

H. Yurimoto, S. Itoh, M. Zolensky, M. Kusakabe,A. Karen, R. Bodnar, Isotopic compositions of asteroidal liquid water trapped in fluid inclusions of chondrites. Geochem. J. **48,** 549-560.

H. Yurimoto, K. Nagashima, T. Kunihiro, High precision isotope micro-imaging of materials. Appl. Surf. Sci. **203-204,** 793-797 (2003)

M.Y. Zolotov, A.L. Sprague, S.A. Hauck, L.R. Nittler, S.C. Solomon, S.Z. Weider, The redox state, FeO content, and origin of sulfur-rich magmas on Mercury. J. Geophys. Res. **118,** https://doi.org/10.1029/2012JE004274 (2013)

M.Y. Zolotov, A.L. Sprague, L.R. Nittler, S.Z. Weider, R.D. Starr, L.G. Evans, W.V. Boynton, J.O. Goldstein, S.A. Hauck, S.C. Solomon, Implications of the MESSENGER discovery of high sulfur abundance on the surface of Mercury. EOS (Trans., Am. Geophys. Union) Abstract # P41A-1584 (2011)

FIGURE CAPTIONS

Figure 1. K/Th and K/U vs. heliocentric distance for the inner Solar System bodies showing the surprising result of Mercury being more enriched in the moderately volatile K than the Moon, Vesta, and possibly the Earth. (Data from Kitts and Lodders, 1998; Lodders and Fegley, 1998; Lucey et al., 2006; McDonough and Sun, 1995; Peplowski et al., 2011; Taylor, 2013).

Figure 2 (a) U vs. La and (b) K vs. La for chondrites and the Earth, Moon, Vesta, and Mars. U and La are both refractory incompatible elements and show that planetary differentiation does

not alter this primordial ratio. The depletion in K of the Earth is very similar to that of CV chondrites. Data from Halliday et al., (1995); Jochum et al., (1991); BVSP (1981); Newsom et al., (1986); Haskin and Warren (1991); Jerde et al., (1990); Joliff et al., (2003); Korotev (1987); Korotev and Kremser (1992); Warren and Kallemeyn (1986); Warren (2005); Kitts and Lodders (1998).

Figure 3. Abundances of the moderately volatile elements and volatile elements vs. 50% condensation temperature for chondrites: (a) CM (b) CO (c) CV (d) LL (e) EH (f) EL. The abundances are normalized to CI chondrites and silicon. Black circles indicate siderophile elements, open circles are lithophile, grey circles are chalcophile, and open squares are volatile. The chalcophile and siderophile elements are already mobilized due to early parent body processes on the LL parent body. Metamorphism has also affected the EH and EL chondrites. Volatile data from Alexander et al. (2012) for Murchison (CM), Mokoia (CO), Kaba (CV), Semarkona (LL). C and N from Grady et al. (1986) for (EH) and (EL), with data for other elements from Wasson and Kallemeyn (1988) and Lodders and Fegley (1998). Dashed grey lines are the moderately volatile element trend of the Bulk Silicate Earth from Palme and O'Neill (2014).

Figure 4. A pH_2O vs. time schematic showing three possible evolutionary scenarios for water on Venus. The green curve denotes an early ocean-rich Venus which was lost early likely due to hydrodynamic escape (Kasting and Pollack, 1983). The orange curve represents a monotonic decline due to continuous loss of hydrogen from the upper atmosphere. The purple curve represents episodic input of volatiles, which takes into account the ability of the mantle to retain non-zero levels of water, and releases mantle volatiles during catastrophic mantle overturn events. This large release would likely release low D/H water (similar to other inner Solar System materials) on a ~500 Ma timescale, which then would be fractionated by atmospheric loss processes to the observed D/H of ~150x terrestrial. Modified from Gilmore et al. (2017).

Figure 5. ^{1}H image of Shergotty meteorite obtained using SCAPS. The upper region is the mineral apatite (Ap); the lower region is maskelynite (Mk), and a sharp grain boundary can be seen between the two phases. Apatite is brighter because it has several thousand ppm wt H_2O,

1808 while the maskelynite is nominally anhydrous (~<100 ppm wt H_2O). The most water-rich phase
1809 in this image is terrestrial contamination along cracks, fractures, and micro-cracks. Typically, a
1810 ~20 μm diameter crack-free area is needed for SIMS analysis. This illustrates the extreme
1811 difficulty in obtaining 'true' martian D/H values in shocked extraterrestrial samples (source: J.
1812 Greenwood, unpubl. data).
1813
1814 Fig. 6. Geophysical estimates of water content and temperature in the lunar interior at the depth
1815 of 800 km. The inferred water content is from 0.01 to 0.001 wt% that is comparable to, or only a
1816 factor of ~10 less than, that of Earth's asthenosphere (0.01 wt%). Modified from Karato (2013).
1817
1818 Figure 7. Seasonal changes in atmospheric water species on Mars. D/H maps on top with
1819 abundance maps of HDO and H_2O below. Figure adapted from Villanueva et al. (2015).
1820
1821

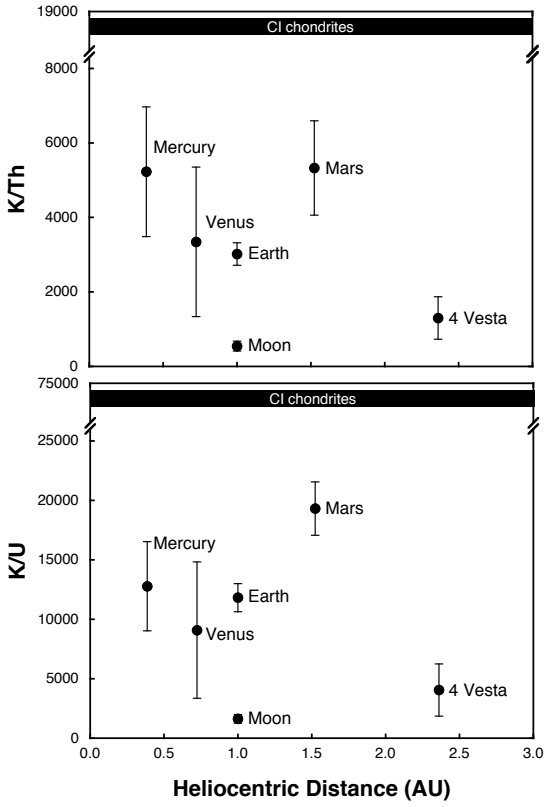

1822

1823

1824

1825

1826 **FIGURE 1**

1827

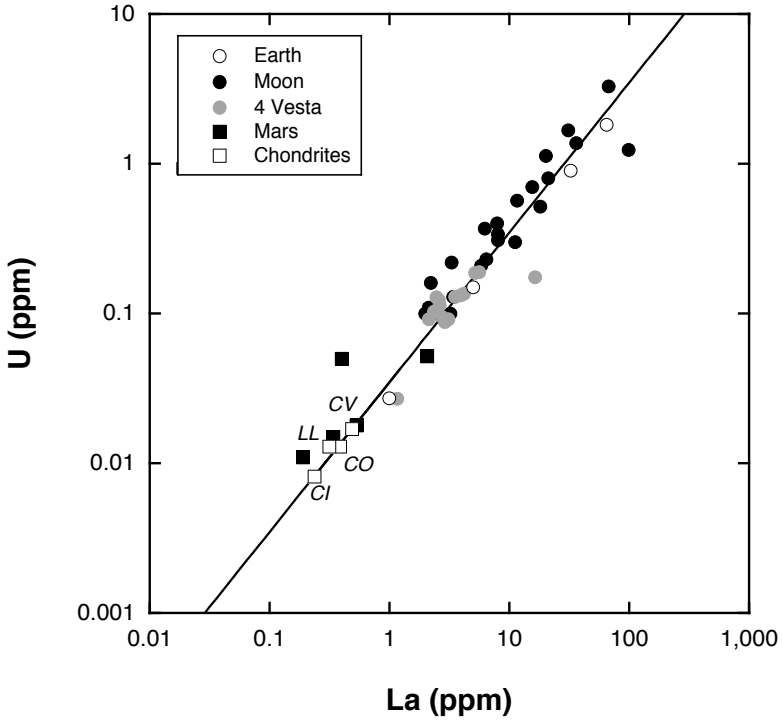

1828

1829 **FIGURE 2A**

1830

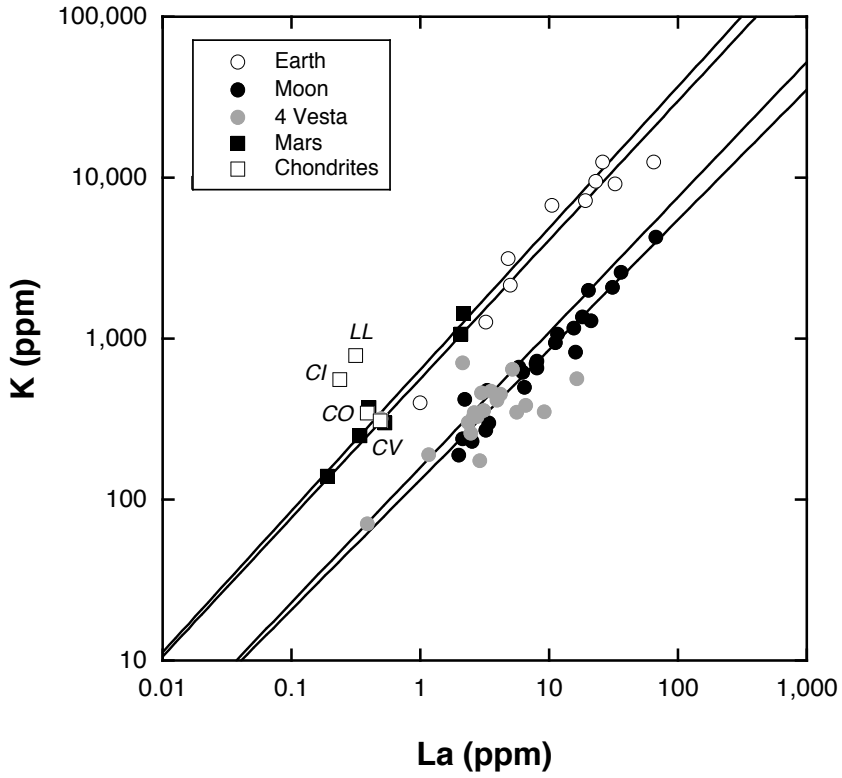

1831

1832

1833 **FIGURE 2B**

1834

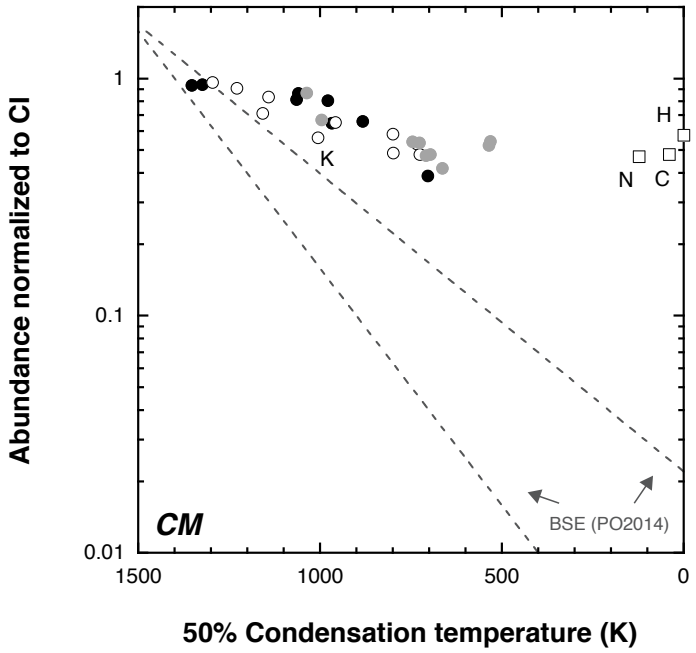
Abundance normalized to CI
1
0.1
0.01
1500
1000
500
0
50% Condensation temperature (K)
CM
K
H
N
C
BSE (PO2014)

FIGURE 3A

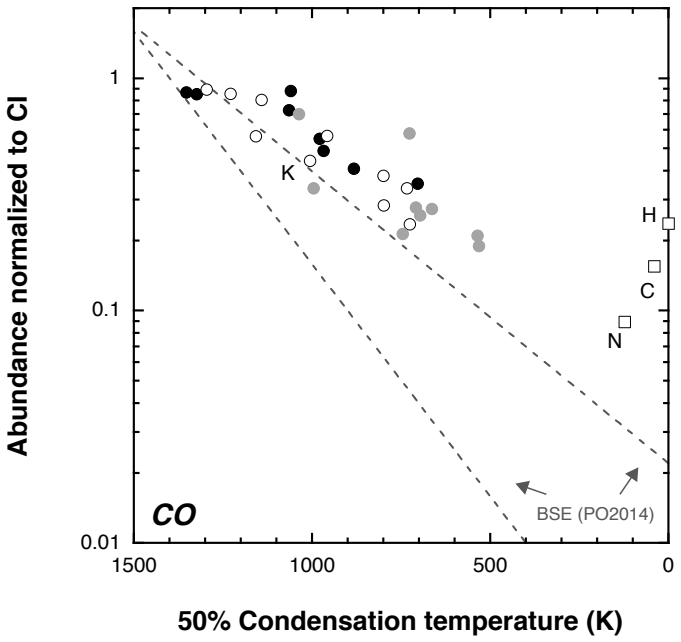
Abundance normalized to CI
1
0.1
0.01
1500
1000
500
0
50% Condensation temperature (K)
K
H
C
N
CO
BSE (PO2014)

FIGURE 3B

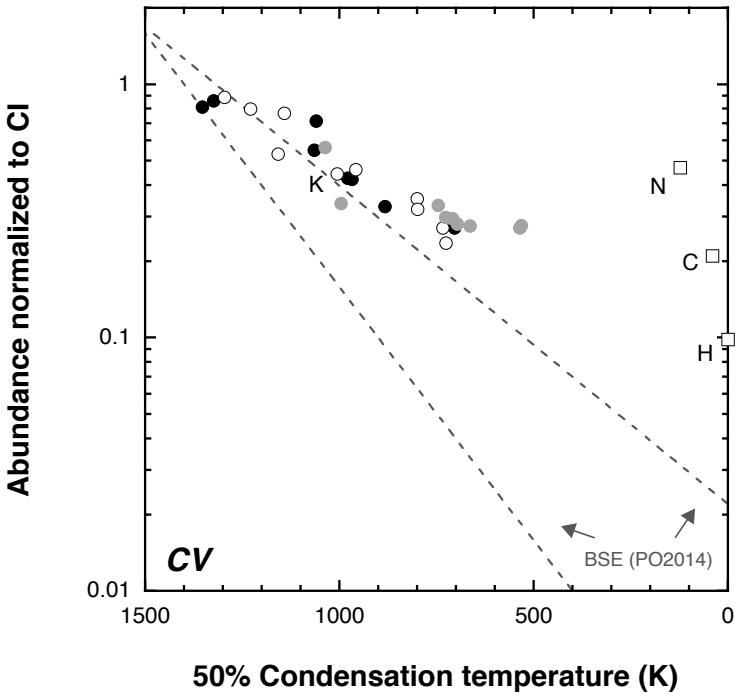
Abundance normalized to CI
1
0.1
0.01
1500
1000
500
0
50% Condensation temperature (K)
K
N
C
H
CV
BSE (PO2014)

FIGURE 3C

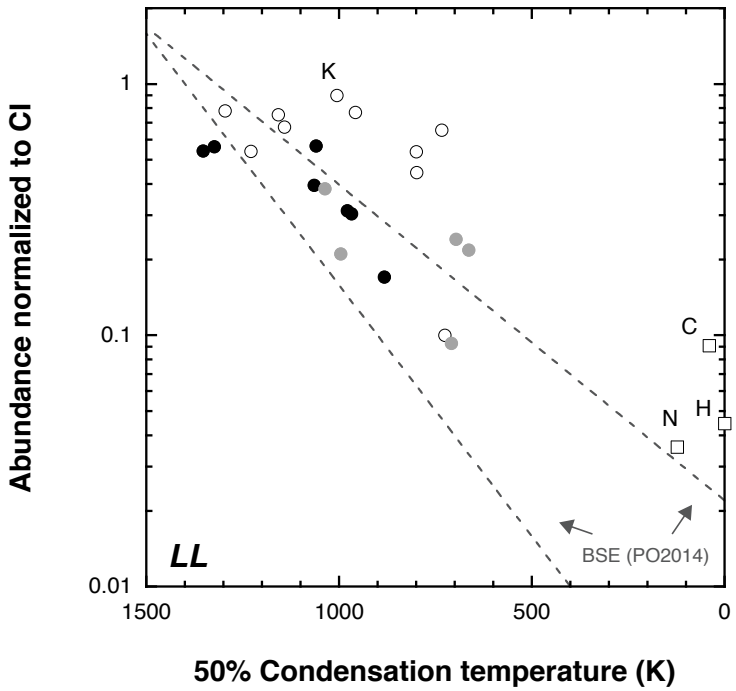
Abundance normalized to CI
1
0.1
0.01
1500
1000
500
0
K
C
H
N
LL
BSE (PO2014)
50% Condensation temperature (K)

FIGURE 3D

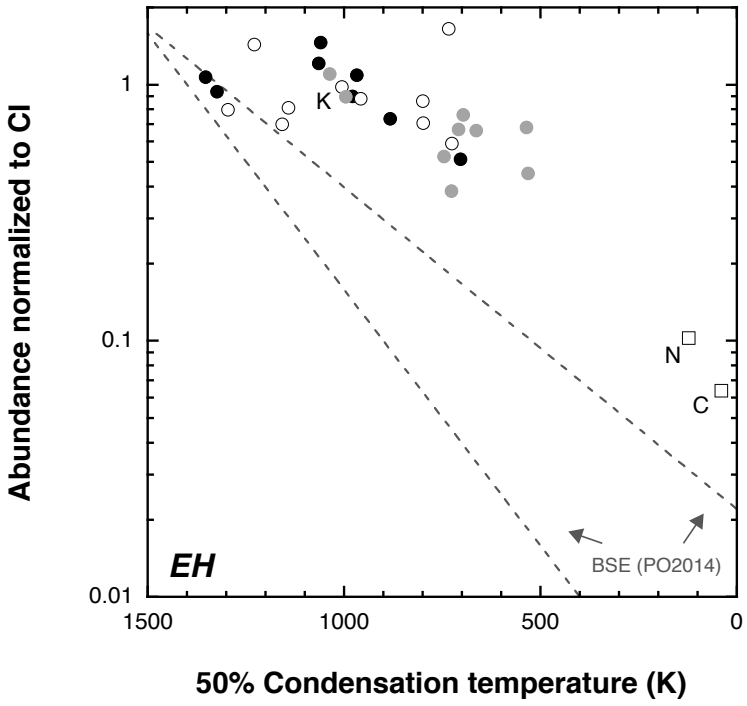
Abundance normalized to CI
1
0.1
0.01
K
N
C
EH
BSE (PO2014)
1500
1000
500
0
50% Condensation temperature (K)

FIGURE 3E

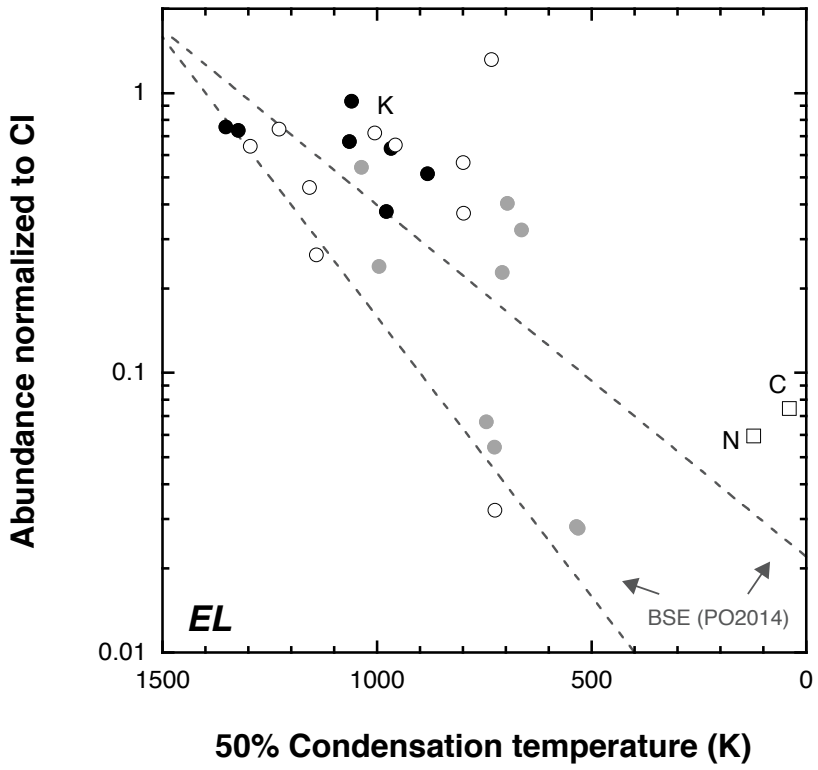
Abundance normalized to CI
1
0.1
0.01
1500
1000
500
0
50% Condensation temperature (K)
K
C
N
BSE (PO2014)
EL

FIGURE 3F

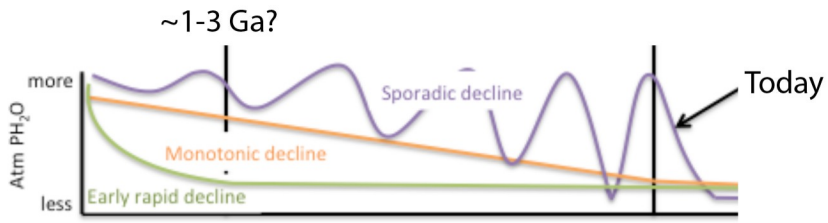
~1-3 Ga?
more
Atm PH_2O
less
Sporadic decline
Today
Monotonic decline
Early rapid decline

FIGURE 4

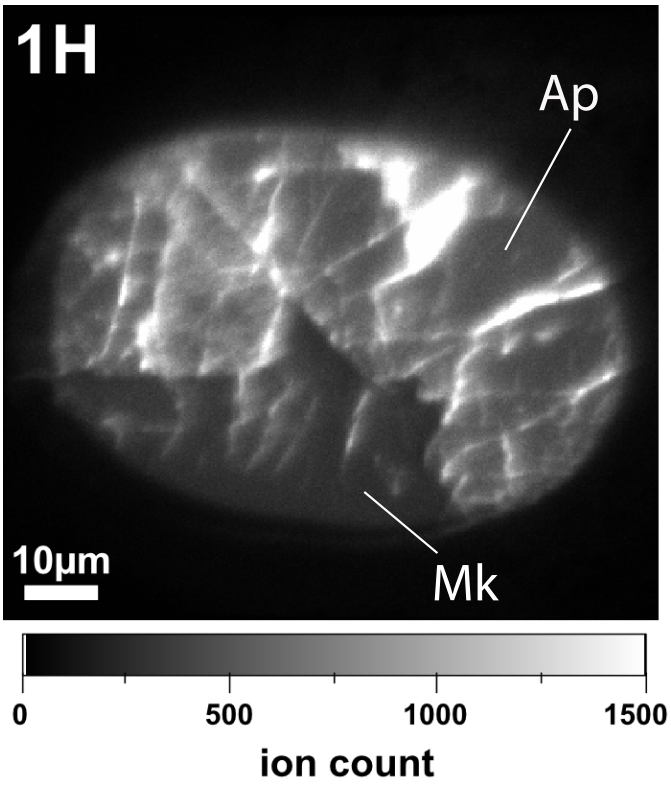

FIGURE 5

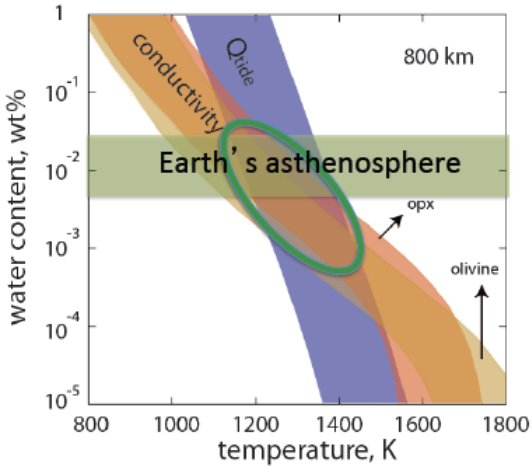
1
10^{-1}
10^{-2}
10^{-3}
10^{-4}
10^{-5}
water content, wt%
800
1000
1200
1400
1600
1800
temperature, K
conductivity
Q_{olide}
800 km
Earth's asthenosphere
opx
olivine

FIGURE 6

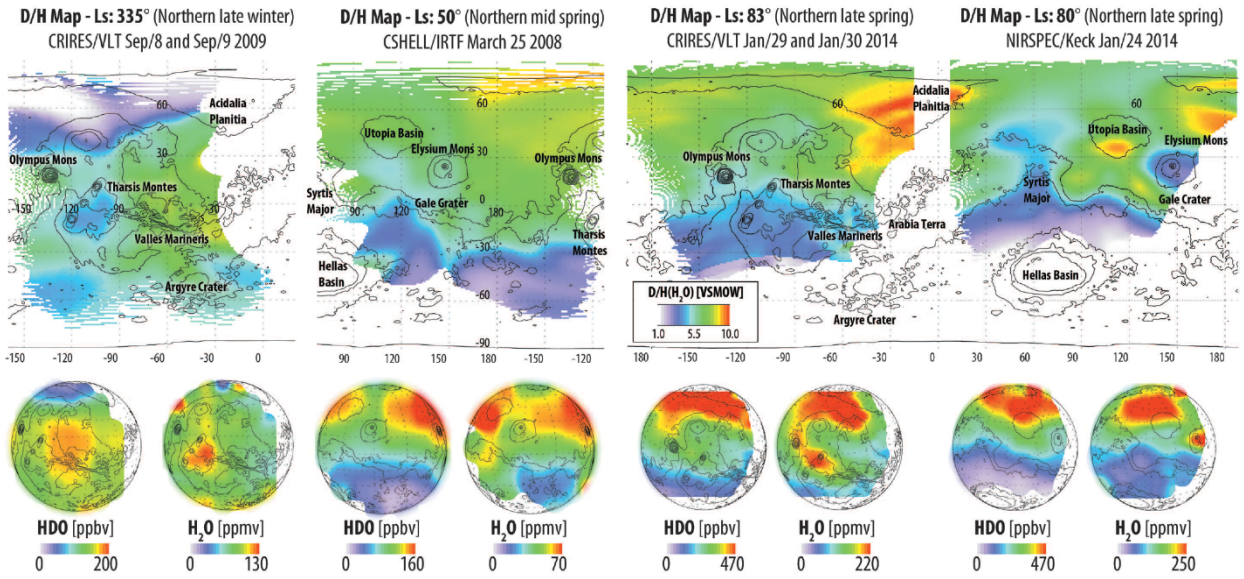
D/H Map - Ls: 335° (Northern late winter)
CRIRES/VLT Sep/8 and Sep/9 2009
D/H Map - Ls: 50° (Northern mid spring)
CSHELL/IRTF March 25 2008
D/H Map - Ls: 83° (Northern late spring)
CRIRES/VLT Jan/29 and Jan/30 2014
D/H Map - Ls: 80° (Northern late spring)
NIRSPEC/Keck Jan/24 2014
Acidalia Planitia
Olympus Mons
Tharsis Montes
Valles Marineris
Argyre Crater
Utopia Basin
Elysium Mons
Syrtis Major
Gale Crater
Hellas Basin
Arabia Terra
D/H(H2O) [VSMOW]
1.0 5.5 10.0
HDO [ppbv]
0 200
H2O [ppmv]
0 130
HDO [ppbv]
0 160
H2O [ppmv]
0 70
HDO [ppbv]
0 470
H2O [ppmv]
0 220
HDO [ppbv]
0 470
H2O [ppmv]
0 250

FIGURE 7